Motivational State Influences the Content of Hippocampal Sequences

by

Alyssa Ashley Carey

A thesis

presented to the University of Waterloo

in fulfilment of the

thesis requirement for the degree of

Master of Science

in

Biology

Waterloo, Ontario, Canada, 2015

Author's Declaration

I hereby declare that I am the sole author of this thesis. This is a true copy of the thesis, including any required final revisions, as accepted by my examiners.

I understand that my thesis may be made electronically available to the public.

Abstract

Hippocampal sharp wave-ripple (SWR) associated sequence activity, commonly referred to as replay, has generally been thought of as mediating the transfer of recent experience into the neocortex. However, a number of recent studies have shown that the content of sequences is not limited to recent experience. To investigate whether internally generated stimuli, such as appetitive motivational states, affect the content of SWR-associated spiking activity, we recorded from ensembles of CA1 place cells while rats were performing a motivational shift task on a simple T-maze. Rats were food restricted or water restricted on alternating days and trained to make a left turn for food and right turn for water. We found that SWR-associated spiking activity recorded prior to task performance was correlated with motivational state and overall behavioural choices, suggesting that it also mediates retrieval of past behavioural episodes to facilitate planning for motivationally relevant outcomes.

Acknowledgements

I truly owe so many thanks. If I were to be deterministic about it—how I ended up here in particular, sitting at my desk with a completed thesis—I may end up thanking everyone I've listed below, everyone else, my distant Australopithecine ancestors that could have went extinct but didn't, the K-T asteroid, the first creature with a notochord, and the Universe—and everything in between, not to mention the gravitational constant.

Data analysis for this thesis heavily relied on code from the vandermeerlab codebase, which mostly comprises contributions from Dr. Matthijs van der Meer and Youki Tanaka. The code used for sharp wave-ripple and multiunit activity detection was written in collaboration with Elyot Grant.

I would like to extend my deepest gratitude to my supervisor, Dr. Matthijs van der Meer, who would be a viable replacement for online research databases after a potential Internet apocalypse. Matt provided valuable discussions, tutorials, and guidance throughout my graduate studies. His 8:30 am undergraduate course, Systems Neuroscience: From Neuron to Brain, inspired my interest in place cells and managed to convert me over to the light phase (at least for Winter 2012). Thank you for providing support and encouragement when I needed it, and most of all for being an excellent mentor.

I am truly indebted to Elyot Grant—my genius companion and dearest friend—who enthusiastically provided math and programming tutorials when I was desperate, fixed that bug I spent 5 hours on in 5 minutes, and wrote a really good SWR detector while watching a Final Fantasy IV speed run on ADGQ. Thank you for tolerating me these past two years. You know what I mean.

I thank my committee members for helpful comments and suggestions: Kari Hoffman (York University), Myra Fernandes (Dept of Psychology, University of Waterloo), and Heidi Engelhardt (Dept of Biology, University of Waterloo).

Thank you to my fellow labmates—past and present—in the van der Meer lab. Hello guys. You're probably not reading this right now. Youki Tanaka, Eric Carmichael, Min-Ching Kuo, Julia Espinosa Grossmann, Julien Catanese, Jimmie Gmaz, and Rob Cross.

I thank various staff at the University of Waterloo. The animal care technicians of the Central Animal Facility provided valuable knowledge and assistance: Nancy, Martin, Jean, and Angela. The machinists of Science Technical Services provided help and suggestions for technical aspects of the experiment. I thank the Biology Graduate Office for all their assistance.

I express my appreciation for all the support from my family and friends, especially Mom and Dad (thanks for investing in a human child, despite not being guaranteed a return on your investment :P), Grandma (for being awesome), Dustyn (my brother, for encouraging me), Evelyn Grant (for feeding me and making me laugh), and Samantha Morrison (for being a great friend throughout).

I would like to irrationally acknowledge my rats who contributed to this research: Cpt. Ratsworth, Dr. Jekyll, Digit, and Obex. Such pretty whiskers.

And finally, I thank caffeine, epic music, and the passage of time.

Wisdom begins in wonder. — Socrates

Contents

List of Figures

List of Tables

List of Abbreviations

ANOVA	analysis of variance
AP	anteroposterior
CA1	cornu ammonis 1
HC	hippocampus
HFE	high-frequency event
IGS	internally generated sequence
LFP	local field potential
ML	mediolateral
MUA	multiunit activity
NAU	number of active units
NCFS	noise-corrected frequency spectrum
OSA	offline sequential activity
SEM	standard error of the mean
SD	standard deviation
SWR	sharp wave-ripple

1. Introduction

1.1 The Hippocampus

The hippocampal formation is an ancient system of brain structures found in most tetrapods (Striedter, 2005). In humans, monkeys, and rats, the hippocampus is important for the rapid acquisition and storage of new information and learned associations. In rats especially, the hippocampus is studied for its role in spatial memory, navigation, and object recognition. Pathologically, the hippocampus is often the site of epileptogenesis and is also an early player in some neurodegenerative diseases such as Alzheimer's.

Early ideas of hippocampal function posited that it was an important memory system (Scoville and Milner, 1957) and contained a cognitive map (O'Keefe and Nadel, 1978). The cognitive map theory was based on an observation that a subset of CA1[1] pyramidal cells were receptive to a rat's location in space (O'Keefe and Dostrovsky, 1971). Such *place cells* have since become one of the most extensively studied neurons of the hippocampus. Although the hippocampus is crucial in spatial memory, rodent place cell firing patterns do not support the idea that it functions as a literal coordinate system (Wood et al., 2000; Dupret et al., 2010; Hollup et al., 2011; MacDonald et al., 2011), or that it encodes spatial information exclusively (O'Keefe and Dostrovsky, 1971; Ranck, 1973; Eichenbaum et al., 1999). Many studies have found that in addition to spatial dimensions, the rodent hippocampus also encodes at least three other dimensions (reviewed in Shapiro, 2015) including time (Eichenbaum, 2014), motivation (Moita et al., 2004, 2003; Kennedy and Shapiro, 2009) and strategy (Ferbinteanu and Shapiro, 2003; Ferbinteau et al., 2011), as well as additional stimuli such as odors, textures, and object locations.

[1] A hippocampal subfield.

1.2 Place Cells and Spatial Encoding

The principal cells of the rodent hippocampus are pyramidal neurons that primarily activate in response to spatial location. Studied extensively in the last four decades as a neural substrate for learning and memory, pyramidal cells encode and store episodes of experience in the hippocampal "memory space" [2](Eichenbaum et al., 1999; Eichenbaum and Cohen, 2014). Many hippocampal pyramidal neurons fire more action potentials in certain locations within an environment, hence their common name: *place cells*[3]. The preferred location of firing is known as a *place field* (Figure 1.1), which is experimentally derived from the tuning curve. For place cells, tuning curves are generated from firing rate maps that form a roughly Gaussian distribution along a two-dimensional horizontal plane[4]. En masse, place fields cover the environment, but not in a uniform or repeating pattern, and overlaps often occur. Place fields take on a variety of sizes, shapes, and behaviours depending on factors such as recording area (CA1 vs CA3), and environmental characteristics (linear track or open platform)(O'Keefe, 2007; Spruston and McBain, 2007).

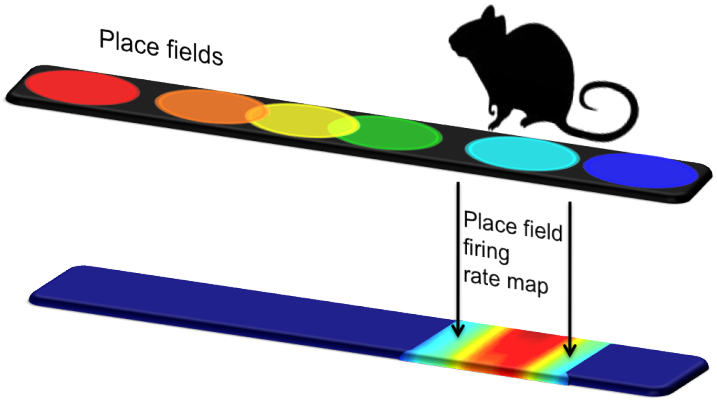

Figure 1.1: Place fields. Top: coloured circles represent place fields along a spatial trajectory. Bottom: The cyan cell increases its firing rate when the animal is inside of the receptive field. This is represented here as a firing rate map with warm colors indicating higher firing rates.

[2]The memory space concept proposes that the hippocampus stores associations between any ethologically relevant dimensions/stimuli experienced in the internal and external environments (Eichenbaum et al., 1999).

[3]But it remains to be determined whether place cells are hiring action potentials to replace the ones they are firing.

[4]Likely owing to the rat's evolutionary history of occupying ground space rather than, say, a three-dimensional air space like bats, which have volumetric place fields (Yartsev and Ulanovskyi, 2013) their place cells fire in columns through a helical runway rather than having unique fields at different elevations (Hayman et al., 2011).

When a rat is actively engaging with its environment, place cells encode many types of stimuli within the environment, such as objects (Larkin et al., 2014), odors (Farovik et al., 2010), and textures (Shapiro et al., 1997). Place cells also encode associations within the environment such as place-fear associations (Moita et al., 2003), and the hippocampus is required for odor-place associations (Tse et al., 2007). The most salient feature that place cells encode is the rat's current location. In fact, if the sample size of recorded neurons is large enough, decoding algorithms can be applied to estimate the animal's actual location in space based on the population activity seen during previous behavioural episodes (Zhang et al., 1998). This strongly suggests that the hippocampus uses place cell activity to encode location. If place cell activity forms the basis of episodic-like memory in rats, we may be able to sample place cells and find—in their observed electrical activity—what may emerge as a memory within the brain. This is often implicit in studies of a phenomenon known as awake replay (described in more detail in upcoming sections), which is speculatively equated to recall of episodic memory in humans. In rats, it is probably more appropriate to think of it as the reinstantiation of past experiences, but some researchers may go further and refer to it as *episodic-like* memory when talking about animals. Briefly, replay manifests as non-local (extrafield) firing of place cells from a previously experienced trajectory, usually while the rat is stationary or quiescent. The animal is not present in the cells' receptive fields while this is occurring, yet the place cells are firing as if the rat was actually running within the environment, albeit at a much faster timescale. In fact, the speed of replay may be up to 20 times faster than the activity seen during the actual experience (Diba and Buzsaki, 2007; Foster and Wilson, 2006; Karlsson and Frank, 2009; Lee and McNaughton, 2002). Replays can occur in the same direction (forward replays) or opposite direction (reverse replays) as the original experience. The concept of a forward replay and how it relates to the original experience is illustrated in Figure 1.2.

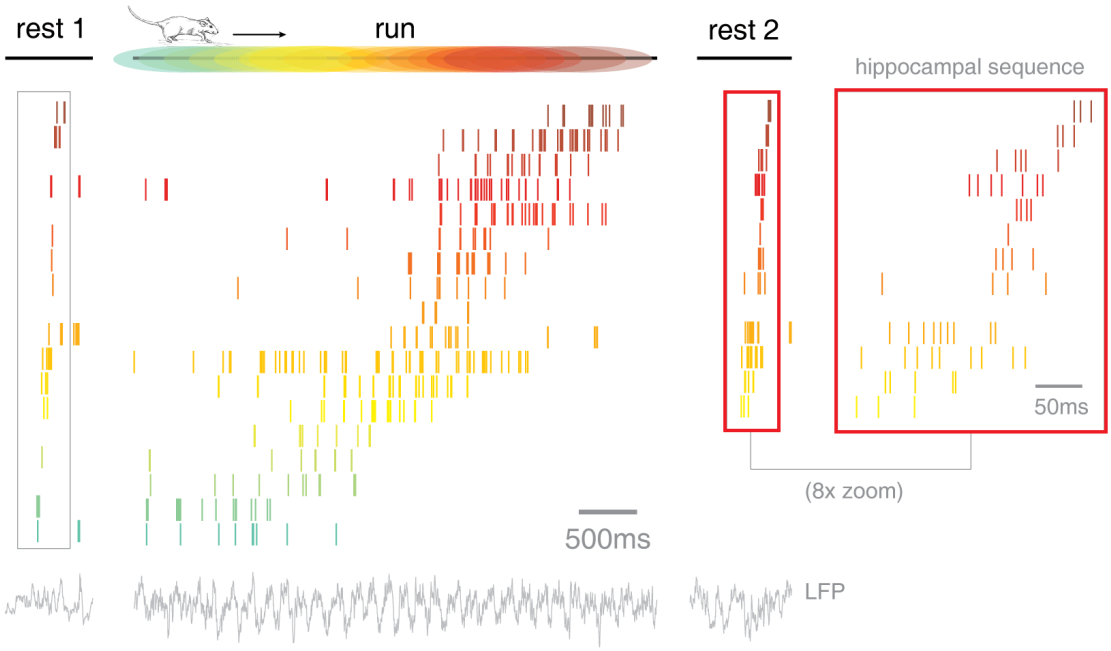

Figure 1.2: Forward replay. Spiking activity of neurons before (rest 1), during (run) and after (rest 2) one lap on a linear track. The direction of travel and relative spacing of place fields, as well as which segment of time represents traversal, is shown above. Each row of coloured tickmarks represents the spikes emitted by different place cells. The spikes displayed in the center represent place cell in-field activity during physical traversal of the track. During the rest periods before and after traversal, there is rapid place cell reactivation mimicking the place field order on the track. These replay events occur during awake sharp wave-ripple complexes. Note the rapid timescale of replay events as compared to the actual experience.

1.3 Hippocampal Anatomy and Circuitry: Place Cells Receive Highly Processed, Multimodal Sensory Inputs

As mentioned previously, place cells are located throughout the hippocampus, which is part of a larger system of structures known as the hippocampal formation. The hippocampal formation is phylogenetically ancient. Its morphology, connectivity and location within the brain are not conserved across species[5], even within mammals (Striedter, 2005). Thus, caution must be exercised when making inferences about human brains based on rodent data since differences in connectivity may reflect differences in functionality.

There is not a consensus as to which structures comprise the hippocampal formation in mammals,

[5] although what constitutes "conserved" is variously interpreted in some rodent papers.

but the dentate gyrus, hippocampus, subiculum and entorhinal cortex are generally included (Amaral and Lavenex, 2007). The hippocampus proper is subdivided into fields CA1, CA2, and CA3. Field CA1 is most easily accessed in the dorsal hippocampus of the rat, and its principal cell layer—stratum pyramidale—is a common target for electrophysiological recordings. The sharp wave-ripple complexes recorded from CA1 likely arise in CA3 (Buzsaki, 1986; Csicsvari et al., 2000). Unlike neocortical regions, which often contain reciprocal axonal projections, the hippocampal formation is predominantly unidirectional (Amaral and Lavenex, 2007). The vast majority of connections to the hippocampus occur with the entorhinal cortex[6], which is somewhat colloquially known as the gateway between the neocortex and the hippocampal formation. The rodent entorhinal cortex receives highly processed, multimodal sensory input from a number of cortical brain structures, which it then processes and sends to the hippocampus and dentate gyrus. The hippocampus, in turn, processes this information, and projects back to the entorhinal cortex which relays information to neocortical areas (Amaral and Lavenex, 2007). However, the hippocampus does send direct projections to areas important in executive functions, such as the medial prefront cortex which is involved in decision making (Griffin, 2015). Through recording from CA1, we can sample the convergence of multimodal information pertaining to memory that is sent to downstream structures after being processed by the hippocampus.

1.4 Place Cells Also Encode Internally Generated Stimuli

Many studies have focused on the external—mainly spatial—encoding properties of the hippocampus. However, the hippocampus also encodes internally generated stimuli, such as fear and appetitive motivational states. Moita et al. (2004) found that the locations of some place cell firing fields were altered when rats underwent contextual fear conditioning, suggesting that internal states affect hippocampal representations of the external environment. However, more relevant to the topic of this thesis is place-cell encoding of appetitive motivational states. It has been demonstrated that the hippocampus is required for contextual memory retrieval in food-restricted and water-restricted rats performing a non-spatial memory task (Kennedy and

[6]The medial portion of the entorhinal cortex contains grid cells which are spatially selective: each cell fires maximally at the vertices of a hexagonal grid, and thus has multiple receptive fields (Moser et al., 2008).

Shapiro, 2004). The task took place on a trident maze consisting of a common central arm and a choice point forking into three arms with different outcomes: food, water, or no reward, each hidden inside of a visually distinct goal box. The locations of each reward outcome varied from trial to trial. The rat had to choose which goal box to approach depending on its appetitive motivational state. Hippocampus lesioned rats were significantly impaired at approaching the restricted substance as compared to controls. Thus, the hippocampus is required for retrieval of memories pertaining to a motivationally relevant outcome.

In a follow-up experiment, the same researchers recorded from place cells while rats were performing the task. Since the locations of the goal boxes changed from trial to trial, the researchers were able to dissociate spatial and motivation-related place cell activity as rats traversed the track. They found that only 11% could be classified as true place cells, while 24% were firing in response to either hunger or thirst motivational states. The remaining 65% of cells had varying responses (in the form of different preferred locations or different firing rates) that were not clearly belonging to spatial or motivational categories exclusively. Some cells exhibited prospective in-field firing on the central arm of the track, meaning they were predictive of the rat's destination in one of the three goal arms. The firing properties of the same population of place cells were comparatively unaffected by a hippocampus-independent random foraging task, suggesting that the memory demands of the trident maze task elicited motivation-dependent coding. The authors conclude that place cell representations are affected by internal motivational states when memory retrieval is required to plan for actions in the environment (Kennedy and Shapiro, 2009). It is currently unknown whether place cells that encode motivation also participate in replays.

1.5 Consolidation, Learning, and SWR-Associated Spiking Activity

Consolidation Consolidation is the process by which new information is integrated into existing memory networks. Consolidation of declarative memories is believed to follow a two-stage process beginning with initial encoding and storage of newly acquired information in the hippocampus, followed by redistribution and stabilization in cortical networks for more permanent storage sometime later (Frankland and Bontempi, 2005; Born and Wilhelm, 2012). This is known as system consolidation and is proposed to occur primarily

during sleep when ensembles of hippocampal neurons (Lee and McNaughton, 2002; Louie and McNaughton, 2001; Wilson and McNaughton, 1994) and cortical neurons (Euston et al., 2007; Qin et al., 1997) reactivate according to prior experience; another type, synaptic consolidation, is proposed to occur during exploratory or wakeful states and functions to strengthen the connections between recently active neurons (Born and Wilhelm, 2012; Dudai, 2004).

As previously introduced, replay [7] is a phenomenon of cell assemblies commonly observed in the hippocampus. Replay events are often the focus of experiments that study consolidation and spatial navigation in rodents. They occur during a local field potential oscillation known sharp wave-ripples (SWR), which last for 30 to 120 milliseconds and have high power in the 150–250 Hz ripple band (Buzsaki, 1986). Replays consist of sequences of spikes that occur in a temporal order reminiscent of prior behavioural episodes. SWRs are most common during slow wave sleep, followed by motionless waking behaviours (Buzsaki, 1986). Thus, it is of no surprise that some of the earliest studies of replay established that it was involved in consolidation of new experiences in the hippocampal memory network. Experience-dependent increases in place cell firing during subsequent sleep episodes (Pavlides and Winson, 1989; Wilson and McNaughton, 1994), point to hippocampal involvment in consolidative memory processing. Place cells that were coactive during spatial exploration were also coactive during subsequent sleep episodes (Wilson and McNaughton, 1994), and the temporal order during experience was preserved during sleep reactivation (Louie and McNaughton, 2001; Skaggs and McNaughton, 1996). Studies that disrupted SWRs during sleep found impairments in performance on spatial learning tasks, implicating SWRs and replay in long-term (or system) memory consolidation (Girardeau et al., 2009; Ego-Stengel and Wilson, 2010).

Learning Replay events occur more often after exposure to new environments or after learning new associations, and decrease in prevalence with experience (Foster and Wilson, 2006; Diba and Buzsaki, 2007; Singer and Frank, 2009; Carr et al., 2011), highlighting the importance of the hippocampus in acquisition and storage of novel information. This observation is also supported by coactivation in that novelty increases

[7] As discussed in an upcoming section, not all events traditionally called "replay" are strict recollections of past experience. However, we will still adopt this term to remain consistent across the existing literature.

the coordination of place cells during the initial stages of learning (Cheng and Frank, 2008). As reviewed in Yu and Frank (2014) awake replays during the task could also be important for spatial learning and consolidation (and memory retrieval, discussed in more detail later), since they are most common at choice points, during behavioural pauses, and at reward sites (Karlsson and Frank, 2009; Davidson et al., 2009; Singer and Frank, 2009; Diba and Buzsaki, 2007). In support of this idea, experiments that disrupted SWRs in awake rats resulted in impairments on spatial navigation tasks (Jadhav et al., 2012), either because this interfered with short-term memory storage or with memory retrieval.

Place cell reactivation does not always occur in the same temporal order as the experience. Reverse replay—which represents the reverse trajectory—preferentially occurs after the first traversal of a track when the animal has paused to consume a reward [8] (Diba and Buzsaki, 2007; Carr et al., 2011) and occurs even when the reverse trajectory has never actually been experienced (Gupta et al., 2010). It may function in linking reward outcome to previous behaviour (Foster and Wilson, 2006; Carr et al., 2011), and is proposed to result from a remnant dopamine signal in recently active neurons, making them temporarily more excitable (Foster and Wilson, 2006), and also explaining the lack of reverse replay during sleep (Lee and Wilson, 2002).

As previously discussed, place cells encode and store memories of spatial experience, re-expressing them during subsequent wakeful and sleep episodes in patterns that follow a similar temporal order. However, recent studies have added additional insights into the function of SWR-associated hippocampal sequences. Namely, that they may also be involved in retrieval of past memory traces and expression of anticipated future trajectories.

[8] *Reverse replay* can be distinguished from *forward replay in the opposite direction* by considering replays containing cells that fire unidirectionally; such unidirectional place cells are common on linear tracks, resulting in different sequences for opposite heading directions (Lee and Wilson, 2002; Foster and Wilson, 2006).

1.6 Beyond Consolidation: Additional Insights into the Function of SWR-Associated Spiking Activity

Experience Alone Does Not Account for All Cases of Replay

Although it is true that the frequency of SWRs increases after exposure to an environment, and that they are more prevalent in new environments, it does not appear that experience is the sole correlate of non-local place cell activity. It has been observed that awake replay does not reflect the immediately previous trajectory experienced by rats, suggesting that replay does not reflect recentness of experience during shorter time intervals (Gupta et al., 2010). The same researchers found that replay of recent trajectories was as prevalent as replay of non-recent trajectories, and proposed that the content of replay might be independent of experience. Furthermore, earlier research found that awake remote replay of a prior, same-day environment was as common as local replay of a different, current environment (Karlsson and Frank, 2009). Thus, the relationship between replay and experience is complicated. Indeed, in addition to its role in memory consolidation, replay may serve a more active function in navigation and could even be goal-directed, at least sometimes.

Retrieval and Planning

In addition to playing a role in consolidation, recent studies have found that SWR-associated sequences may also be important for memory retrieval and planning. Singer et al. (2013) found that the degree of coordinated place cell activity during SWRs predicted future correct choices, implicating SWR-associated spiking in planning. This task required food-motivated rats to alternate which arm they approached on a W-track. Upon leaving the central arm, rats had to recall which arm they had most recently visited and choose the opposite arm. During the initial phase of learning, place cell coactivation was related to correct performance, however this declined as rats became more familiar with the task. This study suggests that SWR-associated coactivity is important both for learning new hippocampus-dependent spatial tasks and for retrieving records of prior experience in order to select or plan the next route.

Pfeiffer and Foster (2013) found that replay-like events were predictive of a rat's future goal-directed route, whether he was foraging for a reward or returning to a home base on a two-dimensional open platform. The researchers recorded from very large neural ensembles, up to 250 units simultaneously, while rats performed a hippocampus-dependent spatial memory task that involved foraging for rewards in hidden wells of a platform. After foraging for a reward hidden in a random location, the rat could reliably find a reward at a home base. SWR-associated sequences encoded trajectories that approximated the path between the rat's current location at a random well and his future destination at the home well. In fact, the trajectories resembled the future path more than they reflected the past path, supporting the findings by Gupta et al. (2010) that recent experience does not account for all cases of replay.

Gupta et al. (2010) also found that memory retrieval might also result in the creation of short-cuts: one rat was able to link trajectories that occurred over different behavioural episodes into a new trajectory spanning the track between two reward sites. Thus, replay-like events may be more than literal recall of episodic memories. In summary, the research presented above has established that awake, local SWR-associated spiking activity can be identified as prospective (in the form of replays or co-ordinated pair activity) in some cases while a rat is performing hippocampus-dependent spatial memory tasks.

2. Research Question, Overview, and Summary of Previous Findings

Question: Do appetitive motivational states affect the content of non-local hippocampal sequences?

In the previous section we discussed important research findings relating to 1. place cells encoding non-spatial dimensions including internal motivational states, and 2. non-consolidative correlates of place cell activity, namely prospective non-local sequence activity. To date, no research has investigated the union of these two findings: whether motivational states influence the content non-local sequence activity.

To summarize relevant findings from previous research, Kennedy and Shapiro (2009) found that the rat hippocampus represents space differently depending on internal motivational state: whether the subject is seeking out a food or water reward. In the authors' words, "hippocampal representations encode the relationships between internal states, the external environment, and action to provide a mechanism by which motivation and memory are coordinated to guide behavior." (Kennedy and Shapiro, 2009). With reference to prospection, two groups of researchers found that hippocampal representations can be predictive of future trajectories in food-motivated rats. The first group, Singer and colleagues (2013), examined SWR-associated coactivation (or co-occurrence) of place cells while rats were performing a spatial alternation task and found that these representations were predictive of future correct arm choices. The second group, Pfeiffer and Foster (2013), examined SWR-associated sequence activity (commonly called replays) while food-motivated rats were performing a goal-directed foraging task and found that these sequences approximated future trajectories more than past trajectories. Therefore, we have evidence that hippocampal place

cells encode motivational states (albeit in-field) for food- and water-motivated rats, as well as future trajectories for food-motivated rats. However, it remains to be determined whether place cells explicitly encode non-local, motivationally relevant representations where alternatives (food and water) are present.

To investigate whether internally generated stimuli, such as appetitive motivational states, affect the content of SWR-associated spiking activity, we recorded from ensembles of CA1 place cells while rats were performing a motivational shift task on a simple T-maze. Unlike Kennedy and Shapiro (2009), who investigated local, in-field activity and required constantly alternating reward locations to dissociate spatial and motivational dimensions, an experiment such as this one requires a consistent and predictable reward location so that rats can plan their trajectories ahead of time. In this experiment, rats were food-restricted or water-restricted on alternating days and trained to make a left turn for food and right turn for water. At the beginning of each experimental session, it had been approximately 20 hours since the rat was last on the track. During an initial wait period, we recorded place cell spiking activity that may correspond to prospective reactivation in the form of cell-pair coactivity or full-fledged replay events. The key measures for assessing the content of the spiking activity are therefore 1. *Z-score co-occurrence*, to test if the joint firing probability of left-only or right-only cell pairs is greater than chance, and 2. *sequence analysis*, to determine if spiking activity is significantly ordered and corresponds to left or right trajectories on the track.

3. Important Terminology

In systems and behavioural neuroscience, the language can become quite dense and pedantic. Here we will explicitly state the hierarchy of terminology specifically as it relates to categories of spiking activity and local field potential (LFP) oscillations used in the literature (see Figure 3.1). Firstly, the hippocampus receives highly processed multimodal sensory information, and it generates *representations* based on this incoming information. When a rat's hippocampus is representing stimuli that are currently occurring, we say that the place cells are exhibiting *local* or *in-field* activity; on the other hand, when his hippocampus is representing past stimuli we say that his place cells are exhibiting *non-local* or *out-of-field* activity. Obviously, to determine whether the rat is exhibiting local or non-local representations we have to 1. record the current activity of his neurons, 2. know his current location, and 3. have stores of past neural activity and how it was correlated to his behaviour and environment at that time.

We record two types of neural activity: 1. the summed electrical activity of all neurons within the vicinity of a recording electrode, known as the *local field potential* (LFP), which consists of time vs voltage data, and 2. action potentials, or *spikes*, which are above-threshold voltages in the LFP represented as single points in time. When place cells spike non-locally, such as during consolidation or retrieval, we consider them to be *internally generated sequences* (IGS) (Pezzulo et al., 2014) because there is not necessarily a direct external stimulus eliciting this response. We often describe IGSs from a spiking perspective and from a LFP perspective combined. For example, we may talk about theta sequences, which are temporally ordered spike sequences that occur during theta oscillations in the LFP, or we may talk about another category known as offline sequential activity (OSA) (Buhry et al., 2011) which includes spikes associated with high frequency (150-250 Hz) oscillations in the LFP. These are further divided into high frequency, high amplitude oscil-

lations in the LFP—also known as sharp wave-ripples (SWRs)—as well as high frequency, low amplitude oscillations. Both of these (high amplitude and low amplitude oscillations) are referred to as high frequency events (HFEs) in this thesis[1] and both can contain sequences commonly referred to as replay events. High amplitude HFEs (or SWRs) are extracted using a higher detection threshold, whereas low amplitude HFEs are extracted using a lower detection threshold. Since we use a lower detection threshold, as described in the methods section, our detected events are referred to as HFEs rather than SWRs. Lastly, when we are speaking of the segments of data that will be analyzed for non-local representations, or the candidate events, these consist of spiking data that is associated with HFEs in the LFP (i.e. only the spike portion is being analyzed). However, for all intents and purposes, HFEs and candidate events can be considered synonymous.

[1]The terminology for HFE was adopted from Cheng and Frank, (2008).

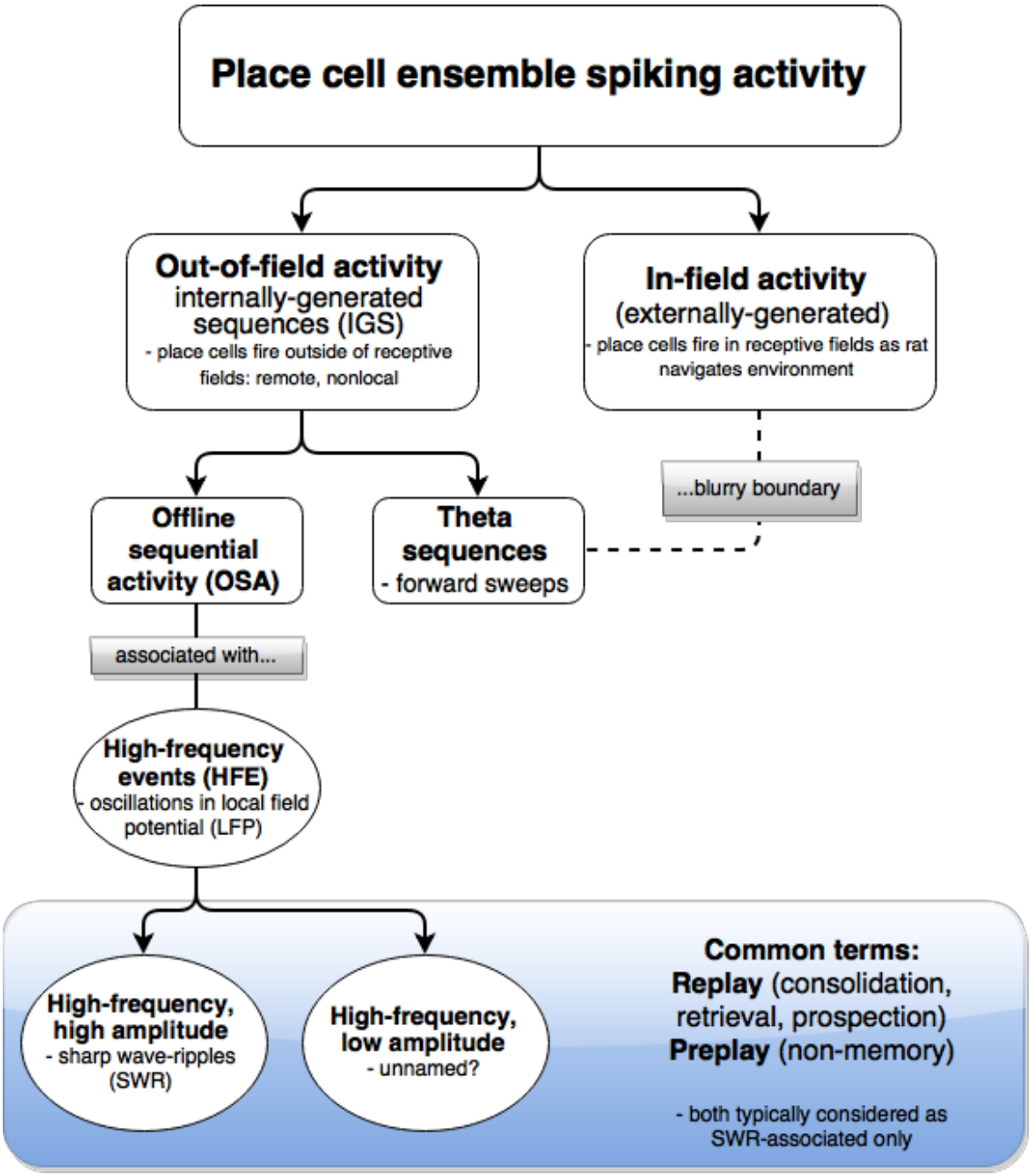

Figure 3.1: Hierarchy of spiking terminology. Place cells spike together as a population, or as ensembles. Ensemble activity is broadly divided into two forms: in-field activity and out-of-field activity (aka internally generated sequences, or IGS). IGS can be further divided into theta sequences which are associated with theta oscillations (and which are not necessarily sharply divided from in-field activity), and offline sequential activity (OSA) which is associated with 150-250 Hz oscillations. OSA, which is a term centered around spiking activity, can be referred to as high frequency events (HFE) with reference to the local field potential. HFEs can be high amplitude, such as SWRs, or low amplitude. Common terms for significantly ordered HFE-associated OSA include replay (forward, reverse) and preplay, as well as less common terms such as trajectory events or whatever best describes the correlates.

4. Methods

4.1 Experimental Procedures

All procedures were performed in accordance with the Canadian Council for Animal Care's policy on the treatment of experimental animals, and were approved by the University of Waterloo's Animal Care Committee, protocol #11-06.

4.1.1 Subjects

Three male Long-Evans rats (Charles River Laboratories and Harlan Laboratories) at least 6 months old were implanted (R042, R044, R050). They were kept in a temperature-controlled environment on a non-reversed, 12-h light-dark cycle. They were housed with two other littermates and provided with ad libitum food (Harlan rodent diet 8640, Teklad Laboratory Diets) until they reached an adult weight of 400 g, after which they were housed separately and maintained on 18 g of food per day. Water was freely available. Rats were pre-handled one week to one month before training began in order to increase familiarity with the researcher. Rats weighed 439–489 g when training began. During experimentation, rats were food or water restricted to no less than 90% of their free-feeding body weight to encourage performance on the task.

4.1.2 Experimental Environment and Behavioural Apparatus

Experiments took place in a windowless room containing a T-maze with associated feeder and water reward systems (Figure 4.1), various supplies, and recording hardware. The behavioural task took place on a wooden, raised, bent-arm T-maze painted black (track dimensions can be found in Figure 4.2). The left arm was painted with thick white stripes for visual distinctiveness from the right arm. The end of the left arm was equipped with a food receptacle attached to a feeder that dispensed 5 food pellets (Test Diet 5TUL, 45 mg each) per approach; the right arm was equipped with a water reservoir attached to a valve that dispensed 0.13 g of 6% sucrose water per approach. Reward dispensing was controlled automatically by a custom written program and triggered when the rat passed a sensor positioned on the corresponding arm. Two movable towel-covered waiting platforms, one on each side of the maze, were positioned between the central arm and reward arms. A black curtain on the North side of the room separated the T-maze from the computer and acquisition system; the remaining walls within the experimental enclosure were exposed. The maze was oriented to face West for R042 and South for R044 and R050[1].

[1]The orientation of the maze was changed from West to South so that the experimental enclosure would be more symmetrical with respect to the goal arms (with the black curtain behind the track rather than on the left side).

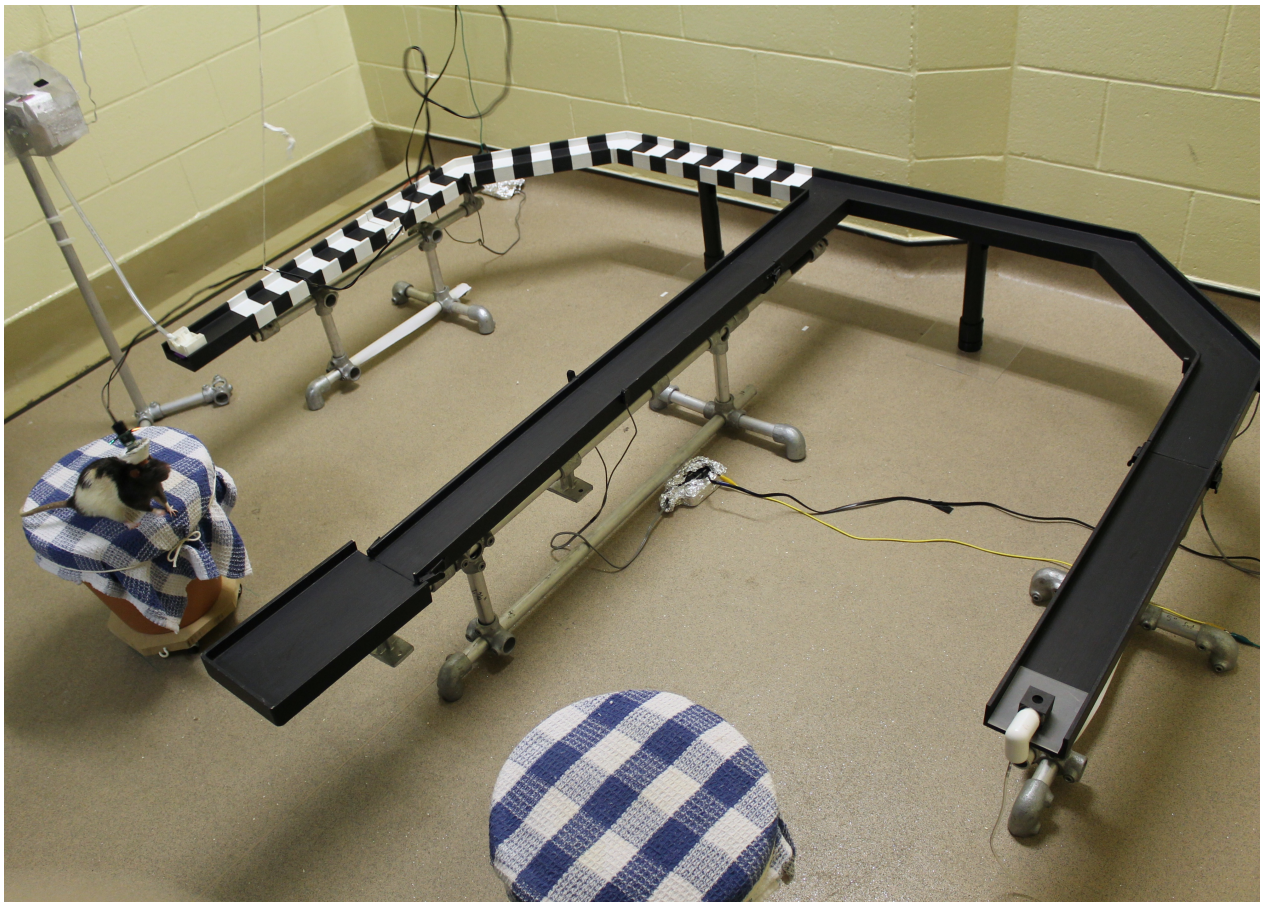

(a) T-maze

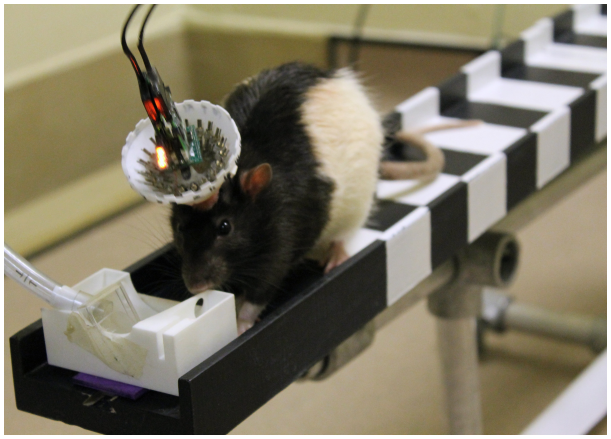

(b) Food receptacle

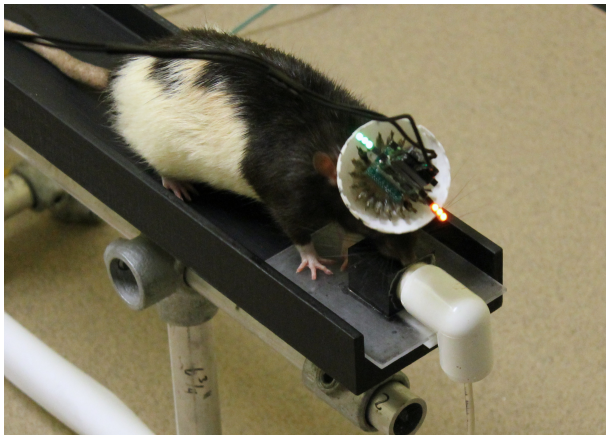

(c) Water receptacle

Figure 4.1: Behavioural apparatus. (a) The T-maze (185 cm x 167 cm) and its associated waiting platforms. The feeder can be seen in the upper left of the image (the water delivery system is partially out of view near the bottom right). The left arm of the track is painted with white stripes for visual distinctness from the right arm. (b) A close-up of the food receptacle at the end of the end of the left arm. (c) A close-up of the water receptacle at the end of the right arm.

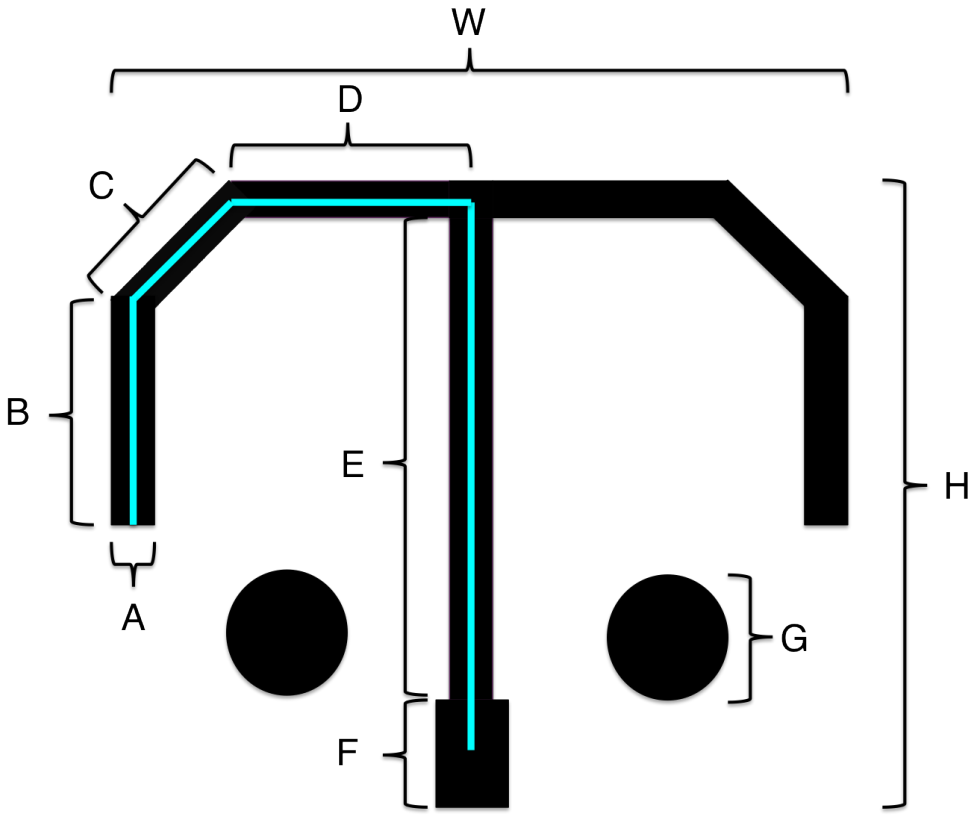

Figure 4.2: T-maze dimensions. A = 10 cm; B = 28 cm (R042), 86 cm (R044,R050); C = 39 cm, D = 60 cm; E = 130 cm; F = 29 cm (not present for R042); G (associated waiting platform) = 35 cm; H (total maze depth) = 167 cm; W (total maze width) = 185 cm. The track is elevated 38 centimeters from the floor, and has short 2.5 cm walls. The pathlength (cyan) is 257 cm for R042, and 334 cm for R044 and R050. Each measurement is rounded to the nearest centimeter.

4.1.3 Behavioural Training and the Motivational T-maze Task

Rats were placed on food and water restriction that alternated daily, and were trained on the motivational T-maze task. Before beginning the task each day, rats were given a small quantity of food (90 mg) and 6% sucrose water (100 mg) to remind them of the available rewards and to devalue the non-restricted reward (Balleine and Dickinson, 1998). Then they were placed on a T-maze-associated waiting platform for a 5–20 minute waiting period[2]. They were trained over a period of at least 4 days to make a left or right turn at the choice point for food or water, respectively. A handheld barrier was used to prevent movement in the reverse direction. Rats were allowed to remain at the end of the goal arm until the reward was consumed, or until it was clear that the rat was not interested in the reward, before being transferred to the nearest movable[3] waiting platform where they remained until the beginning of the next trial. Each intertrial period began at a length of two minutes, and decreased with each trial to as short as one minute or less. A stationary barrier was placed at the choice point during some trials in order to force the rat down the unfavoured arm a minimum of five times per session so that place fields can be estimated for both sides of the track. Training occurred in a fully lit room during the light phase. All rats received a minimum of 4 days of training on the Motivational shift T-maze task before implantation. See Table 4.1 for a summary of the session schedule for each rat.

[2]During training, the pre-task waiting period was extended over sessions until it reached the full waiting period that would be used during data collection.

[3]The waiting platforms had wheels, allowing the rat to be transported without being lifted by the researcher.

Table 4.1: Handling, training, recovery, and recording schedule for each rat. Units are number of days.

Rat ID	Prehandling	T-maze pretraining	Recovery (postsurgical)	T-maze retraining	T-maze recording
R042	6	11	4	2	6
R044	6	6	6	0	8
R050	12	4	8	1	8

4.1.4 Microelectrode Array

Extracellular recordings of action potentials and LFPs were performed in part using a chronically implanted microelectrode array (Figure 4.3) with 16–20 independently movable tetrodes, designed and fabricated in-house. Each tetrode was made of four twisted, heat-fused, $13\,\mu\mathrm{m}$ nichrome wires, and soldered into a Neuralynx EIB-36-16TT interface board. Each channel was tested for cross connections, verified for impedance, and automatically electroplated in gold chloride using a nanoZ. Final impedances ranged between 250–$380\,\mathrm{k}\Omega$. Arrays were enclosed in a 3D-printed cone and cap system before implantation and weighed 20–25 g in total.

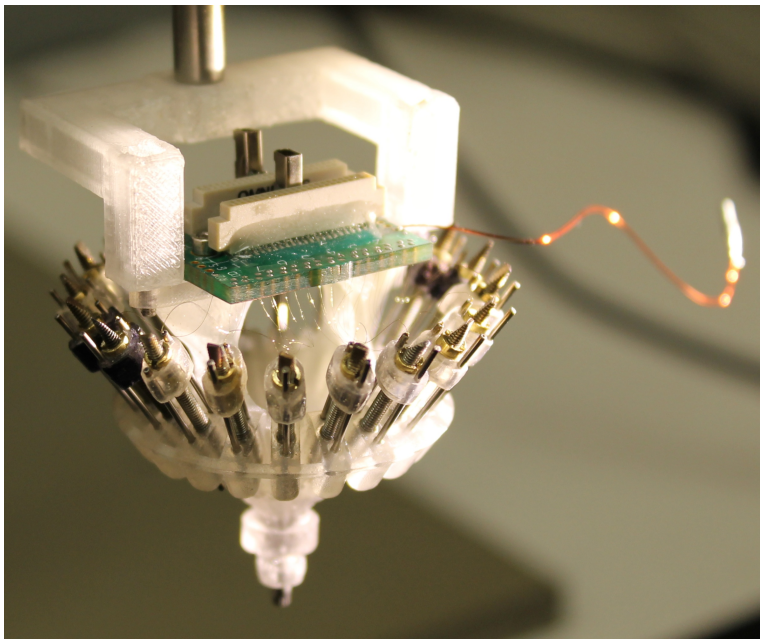

Figure 4.3: Microelectrode array. This array consists of 20 shuttles fixed to a lightweight 3D-printed core, radially arranged around an interface board (green) at the center. Each shuttle is independently movable, and contains one tetrode that extends through a cannula encased in acrylic cement to the bundle (out of focus) at the bottom. The bundle (diameter = $1.8\,\mathrm{mm}$) contains 20 cannulae. Tetrode channels, each much finer than a human hair, are barely visible extending from the shuttles to the board. The ground wire is red. A sterotaxic arm with an adapter piece (white) is holding the array in preparation for electroplating.

4.1.5 Surgery

Subjects (at least 6 months old, weighing 488–525 g) were each implanted with a single-bundle microelectrode array targeting the CA1 region of dorsal hippocampus in the right hemisphere (AP -4.0mm, ML +2.5mm)[4]. R042 and R044 were implanted with 15-tetrode 1-reference arrays, and R050 was implanted with a 16-tetrode 4-reference array. A ground screw was placed through the contralateral parietal bone. The array was lowered to the surface of the cortex, and the remaining exposed opening was sealed with a silicone polymer (KwikSil). Arrays were anchored to the skull using small screws and acrylic cement. Rats were given a minimum recovery period of four days, during which antibiotics and analgesics were administered to minimize postoperative suffering, before retraining began. Tetrodes were slowly advanced to the CA1 layer over a period of 6–9 days. The first recording sessions began no sooner than nine days after surgery.

[4]The right hemishere was chosen because it is a more common target in the rat literature than the left hemisphere.

4.1.6 Recording

Neural activity from all tetrodes and references was recorded on a 64-channel Neuralynx Cheetah data acquisition system. Local field potentials were continuously sampled at 2 kHz, and recorded relative to a reference located in the corpus callosum for removal of muscle artifacts. Spike waveforms were sampled at 32 kHz for 1 ms when the voltage exceeded an experimenter-set threshold and sorted offline. A video tracking algorithm recorded the rat's position based on headstage LEDs picked up by an overhead camera. Additional data consisted of event timestamps, triggered when the rat passed between sensors positioned on the left, center, and right arms of the track. Recording sessions consisted of a 15–25 minute prerecording segment, during which rats were stationed on a T-maze-associated waiting platform, followed by 40 minutes of the Motivational T-maze task, and finally 15 minutes of postrecording on a waiting platform (Fig 4.4).

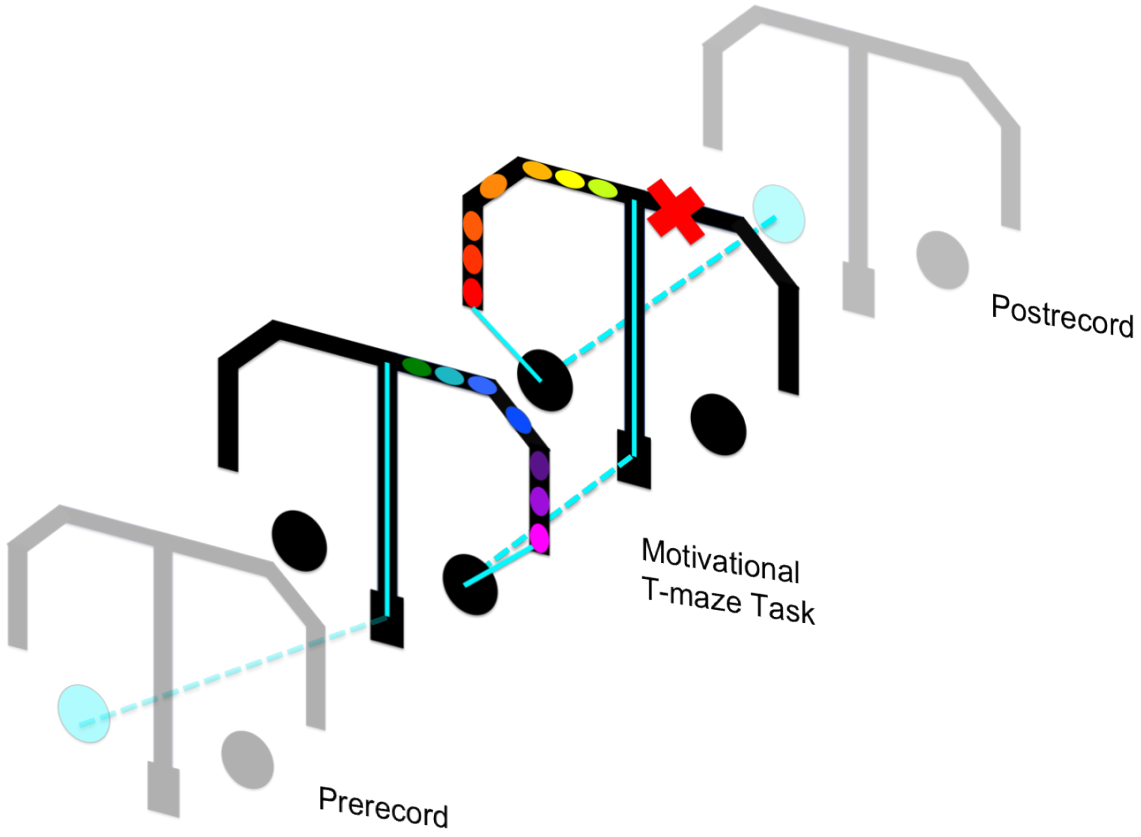

Figure 4.4: Motivational T-maze task and data collection. Rats are stationed on a waiting platform (black circles) for an initial period of 25 minutes (the prerecord) while we record neural activity prior to task performance. Then, rats perform the motivational T-maze task for 40 minutes. They are shuttled to the track where they can choose to make a left turn for food or right turn for water. In order to estimate place field locations for the unfavoured arm, we block the favoured arm at least five times during the task (red X). Place fields are conceptualized as coloured circles. Upon completion of each trial, the rats are transferred to the nearest waiting platform for a intertrial period of 30 seconds to 2 minutes. Rats complete an average of 20 trials per session. After task performance, neural activity is recorded for 15 minutes on a waiting platform (the postrecord). Rat trajectories along the track and through time are represented by a solid and dashed cyan line.

4.1.7 Gliosis, Perfusion, and Histology

After data collection, tetrode sites that recorded both spikes and SWRs in the local field potential were electrolesioned to produce gliosis marks[5]. Two channels per electrode were given 10 µA of current for 7–10

[5]Electric current destroys tissue in the vicinity of the electrode tip, and over the process of 4–5 days is replaced with glial cells that stain darkly relative to surrounding tissues, allowing the tetrode position to be easily discriminated. Otherwise, the gliosis marks

seconds in R042 and R044; all channels of the electrode were given $10\,\mu A$ of current for 5 seconds in R050. References were gliosed with a current of $10\,\mu A$ for 5 seconds in R050 to verify positioning in the corpus callosum and fissure.

At least four days later, rats were anesthetized with isoflurane and euthanized with CO2. They were perfused transcardially with saline followed by 10% buffered formalin. Brains were cryopreserved in a solution of 30% sucrose and buffered formalin for a minimum of 7 days before being coronally sectioned with a cryostat or freezing microtome. To verify placement of gliosed tetrodes in stratum pyramidale of dorsal CA1, brain slices were stained with thionin for contrast and observed microscopically (See Figure 4.5).

result in a zone of clearing if the healing process is not completed before euthanasia.

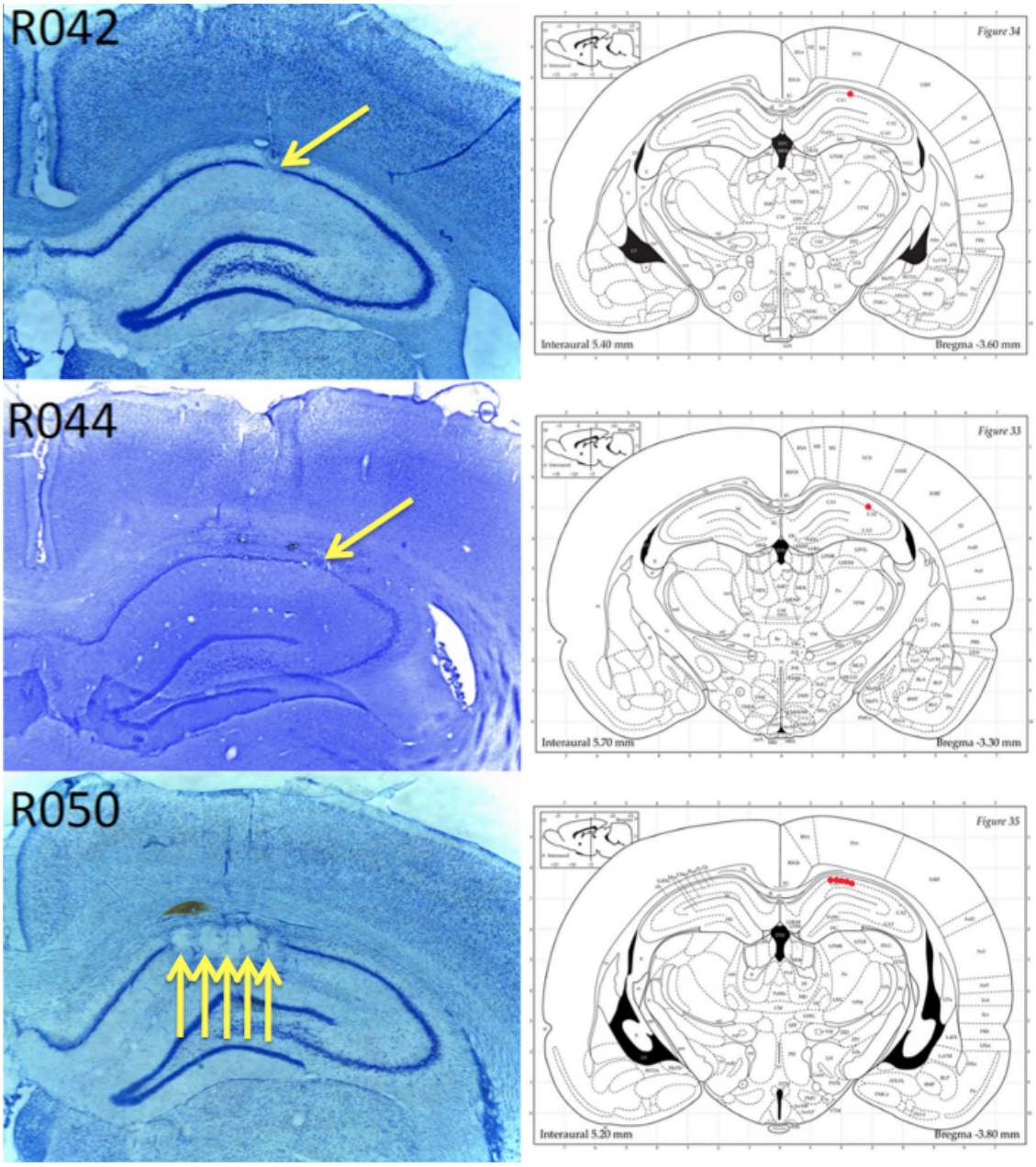

Figure 4.5: Histology. Representative slices verifying tetrode positioning in stratum pyramidale in dorsal CA1 of the hippocampus. Thionin-stained coronal slices are shown on the left, beside diagrams of the rat brain with a red marker where the tetrodes were positioned when they were in the layer. The slice for R042 (top panel) shows a gliosis mark above stratum pyramidale, but the layer itself is broken verifying that the tetrode had been positioned there. R044 has a gliosis mark in the layer along the border between CA1 and CA2. R044's image was edited to improve contrast but did not undergo any other digital alterations. The slice for R050 (bottom) shows gliosis marks for five tetrodes simultaneously. Each slice shows evidence of tetrode tracks passing through the cortex above hippocampus.

4.2 Data Analysis

Data analysis was performed using custom-written programs in MATLAB[6]. The software toolbox FieldTrip (Oostenveld et al., 2011) was used to compute power spectral densities and plot spectrograms.

4.2.1 Preprocessing

Before data can be used for analysis, it must undergo some preparatory preprocessing steps, some of which are unique to some rats or some experimental sessions. Before spike sorting, spiking data for R042 was restricted to exclude regions likely to contain chewing artifcats caused by the jaw muscles, as this rat did not have a reference electrode in the corpus callosum. Some R044 sessions had high-amplitude detachment events[7], thus the spiking data was restricted to exclude these artifacts. In addition to the spiking data restriction, LFPs for the same R044 sessions were restricted to exclude regions where the voltage exceeded 1.5 mV indicative of detachment events.

All spiking data was initially sorted into putative neurons automatically (KlustaKwik, K. D. Harris) and then manually checked and sorted (MClust, A. D. Redish) based on peak voltage, waveform characteristics, and separation in 5 dimensions. Highly unstable cells[8] were excluded from analysis, as well as cells with fewer than 100 spikes during the session, and cells with poor isolation statistics.

4.2.2 Event Detection

The standard procedure for sharp wave-ripple detection typically involves bandpass filtering the signal between 150–250 Hz and using the Hilbert transform to obtain the signal envelope, which is then squared to

[6] Author unlocked new ability: MATLAB.

[7] caused by headstage-array interfacing issues wherein the acquisition hardware became transiently unplugged from the microelectrode array.

[8] Unstable cells have peak voltage that changes dramatically over time, caused by the electrode moving relative to the brain tissue.

obtain the power envelope, and thresholded at 3–5 standard deviations above the mean. Candidate replay events may consist only of detected SWR intervals, but in other cases they may also include regions associated with multiunit activity (MUA)[9]. Here, we use an improved approach[10] for detecting SWRs, outlined in the following sections, and combine this with MUA detection in order to improve the yield of candidate replay events.

Event detection method overview

Briefly, sharp wave-ripple detection is performed by comparing the spectral content of manually identified SWRs to the spectral content of regions of LFP. The result is a similarity score vector, identifying regions of the LFP which resemble SWRs in frequency content. In a separate step, localized regions of multiunit spiking activity are quantified and undergo adaptive thresholding to produce a MUA score vector. Then, the geometric mean of the two scores (SWR and MUA) is taken and thresholded to produce the initial pool of events. Speed and theta power thresholding are used to reduce the number of false positives, and events with fewer than 5 active units are excluded from further analysis (Figure 4.6).

Sharp wave-ripple detection

Manual identification of SWRs Estimating the spectral content of SWRs began with manually identifying 50 SWRs for each session using an 80 ms window. As an extra precaution, SWRs from a representative tetrode channel were identified for each session separately, though this is not necessary to identify SWRs—spectral content is highly similar across different recording sessions and even across different subjects. SWRs were chosen based on features that could easily be judged by eye. Criteria for choosing SWRs included a well-defined, high-amplitude ripple relative to other SWRs recorded during the session, association with

[9] "Neural unit" is a cautious way of saying "neuron" since we cannot know for sure that each cluster of spikes represents all the output from a single neuron. Multiunit activity is thus the spiking activity from many neural units.

[10] The standard procedure failed to detect some regions of the LFP that were clearly associated with replay events. The improved method has fewer false negatives.

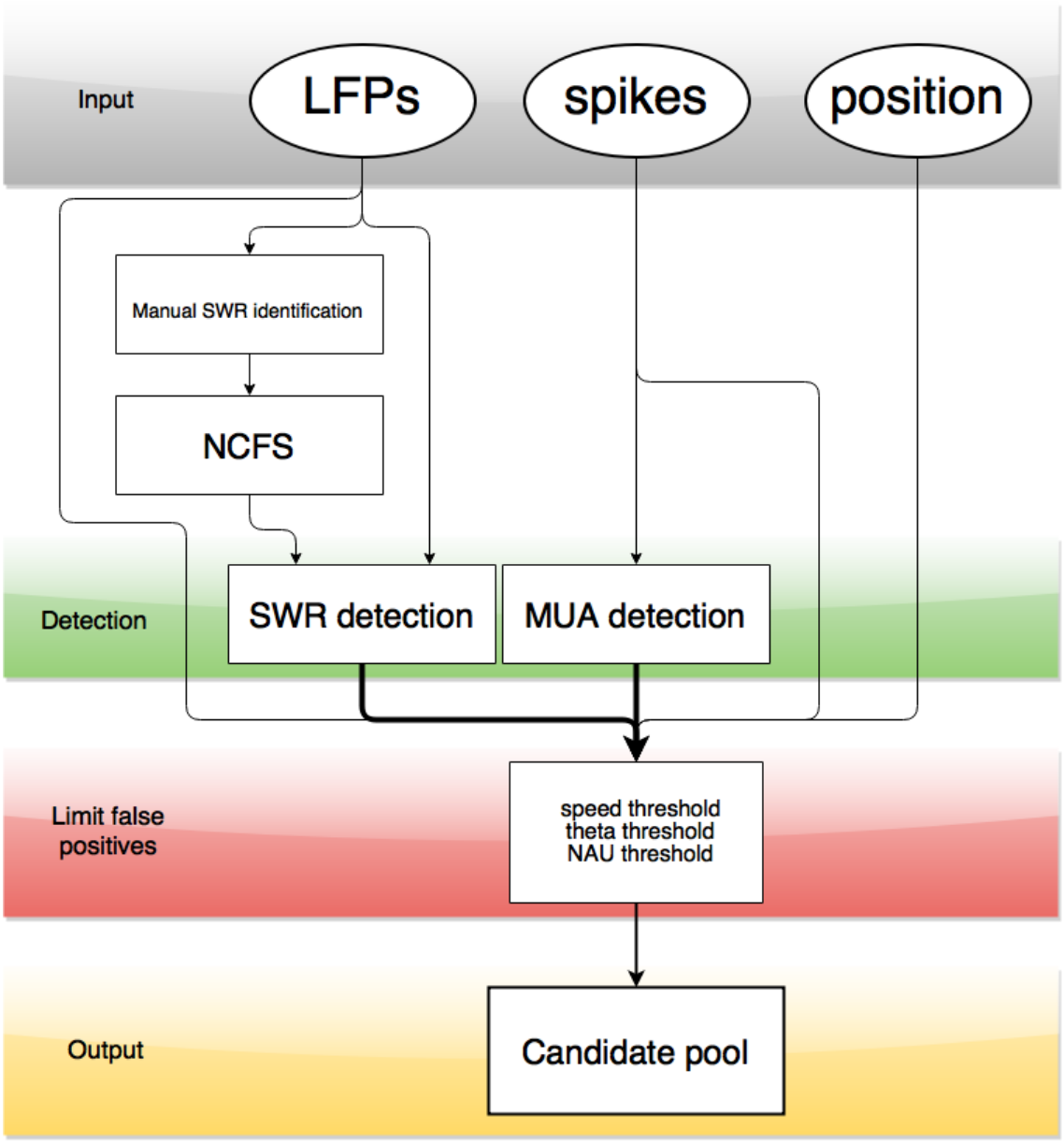

Figure 4.6: Workflow for candidate event detection. Sharp wave-ripple (SWR) detection begins with manual identification of real SWRs in the local field potential (LFP). These SWRs are used to create the noise-corrected frequency spectrum (NCFS), which is then used to automatically identify potential SWRs from the original LFP. At the same time, spike trains (spikes) are summed from all neural units in multiunit activity (MUA) detection. Since the detectors also find regions where theta-sequence activity occurs, the output is limited by speed thresholding (requires position information) and theta power thresholding (requires LFP). Finally, we discard any events during which the number of active units (NAU) is less than 5 (requires spikes). The remaining candidates form the candidate event pool, from which we draw our on-track candidate replays and perform co-occurrence analysis.

spiking activity from multiple units, and a minimum duration of 50 ms.

Generating the noise-corrected frequency spectrum The noise-corrected frequency spectrum (NCFS) describes the relative difference in frequency content between SWRs and hippocampal background noise: Fourier coefficients for the manually identified SWRs were computed using a 60 ms time window, summed (element-wise), and then convolved with a narrow 5-point smoothing kernel ([0.1,0.2,0.4,0.2,0.1], 5 samples at 2 kHz is roughly 2.5 ms). Fourier coefficients were also computed for hippocampal background noise, arbitrarily defined as occurring 2 seconds after each manually clicked SWR on the same tetrode channel, and underwent the same summing and convolution steps. Then, the NCFS was generated by subtracting the noise coefficients from the SWR coefficients (Figure 4.7, and also Figure 4.8, panels A-C).

Identifying SWRs in the local field potential Next, the NCFS were used to identify regions of LFP with similar spectral content, and thus likely to contain SWRs (see Figure 4.8, panels D-I). This involves running the Fast Fourier Transform on a 60-ms time window from the LFP, centered at each data point. The resulting set of Fourier coefficients for each viewing window is given a high pass cutoff of 100 Hz, and then undergoes element-wise multiplication with the noise-corrected frequency spectrum. Then the sum of all elements in the resulting array is taken and used as a score (scalar) for the data point at the center of the current viewing window. Effectively, we take the dot product of the NCFS and Fourier coefficients. This is performed for each data point, and the result is a SWR similarity score vector, that contains regions of high values where the surrounding frequency content in the LFP resembled the frequency content in the manually identified SWRs, and low values elsewhere.

Multiunit activity detection

Multiunit activity (MUA) detection identifies localized regions where multiple cells are active at at the same time. Such regions are often associated with, but not limited to, sharp wave-ripple complexes.

Spikes from all isolated cells are binned into 0.5 ms time bins, producing n vectors (where n is the number of cells), each containing values proportional to firing frequency. Each vector $s(t)$ is convolved with a Gaussian kernel ($\sigma = 40$ samples, or 20 ms) and thresholded (β, described in Equation 4.1) to limit the contribution from individual cells. The n vectors are then summed together to a produce a single score vector $S(t)$ describing raw multiunit activity across the recording session (Equation 4.2; Figure 4.9, panel A).

$$\beta = \frac{2}{\sigma\sqrt{2\pi}} \tag{4.1}$$

β is the *cell activity cap*, a threshold that limits the contribution a single cell can have in determining regions of multiunit activity. $\sigma\sqrt{2\pi}$ is a normalizing factor.

$$S(t) = \sum_{i=1}^{n} min(s(t) * g(k, \sigma), \beta) \tag{4.2}$$

$S(t)$ is the raw multiunit activity detector (before adaptive thresholding). $s(t)$ is the contribution of a single cell to the overall detector. $g(k, \sigma)$ describes a k-point Gaussian distribution with standard deviation σ (k = 200; σ = 40).

Since the MUA associated with SWRs tends to stack in localized regions, whereas the MUA associated with theta sequences tends to be more diffuse and span longer regions, the next step uses adaptive thresholding $A(t)$ (calculated as outlined in Equation 4.3) to limit the amount of theta-sequence activity detected. Essentially, this involves comparing the activity of all regions to the activity of their neighbouring regions: if a region and its neighbours all have a similarly high degree of activity, the adaptive thresholding decreases the MUA score $M(t)$ for these regions (Equation 4.4; Figure 4.9, panel B). The result is that the MUA score gets pulled down for diffuse cell activity relatively more than for stacked cell activity.

$$A(t) = \min(S(t), 4\beta) * G(k_2, \sigma_2) \tag{4.3}$$

$A(t)$ is the adaptive thresholder. The term 4β is the *weighted noise floor*, which pulls $S(t)$ down in regions with lots of spiking activity. $G(k_2, \sigma_2)$ describes a k_2-point Gaussian distribution with standard deviation σ_2 (k_2 = 3000; σ_2 = 250).

$$M(t) = \max\left(0, \frac{S(t) - A(t) - \beta}{\overline{S}}\right) \tag{4.4}$$

$M(t)$ is the multiunit activity detector. $\overline{S}$ is the mean of $S(t)$.

Combining the detectors

The final step of detection involves combining the two detectors (SWR and MUA) by taking their geometric mean (Equation 4.5). The resulting final detector $D(t)$ is unitless and contains higher values in regions that have high SWR similarity and/or MUA activity.

$$D(t) = \text{geometricmean}(R(t), M(t)) \tag{4.5}$$

$D(t)$ is the final HFE detector. $R(t)$ is the sharp wave-ripple detector and $M(t)$ is multiunit activity detector.

A threshold value of 4 was chosen after extensive visual evaluation because it provided a suitable tradeoff between false positives and false negatives[11]. Thresholding produces a preliminary set of intervals—the precandidates—which undergo subsequent limiting steps to reduce the number of false positives. The thresholding produces intervals containing both high-frequency, high-amplitude (SWR) events and high-frequency, low-amplitude events. Some HFEs have relatively low amplitude, but also have associated spikes that form clear replay events. This points to a parallel problem about classifying and detecting replays, which have traditionally been considered a unique phenomenon to high-amplitude (or high-power) SWR events (mentioned in Cheng and Frank, 2008). This is a separate issue that will not be addressed in this thesis. Nevertheless, we chose a threshold that was inclusive for these events and, thus, the pool of candidates may include HFEs that are not considered SWRs. For this reason, candidate replay events will be referred to as HFE-associated rather than SWR-associated.

[11] False positives are segments of data that are not HFEs but were detected anyway; False negatives are segments of data containing HFEs that were missed by the detector.

Limiting false positives and producing the pool of candidate events

Regions of the LFP corresponding to theta sequences can have similar high-frequency spectral content as SWRs, so they are detected by the SWR detector to some degree. Furthermore, they also have associated multiunit activity that is not entirely removed by adaptive thresholding. For this reason we limit the precandidates by theta power thresholding (5–10 Hz, Hilbert transform, maximum 2 SD above mean) and speed thresholding[12] (maximum head speed, 4 cm/s per second). Two additional steps limit the output based on interval duration (minimum 20 ms) and number of active units (minimum 5). The remaining intervals comprise the *candidate events*, which are used in subsequent analyses.

[12]Hippocampal theta oscillations often occur when the rat is moving.

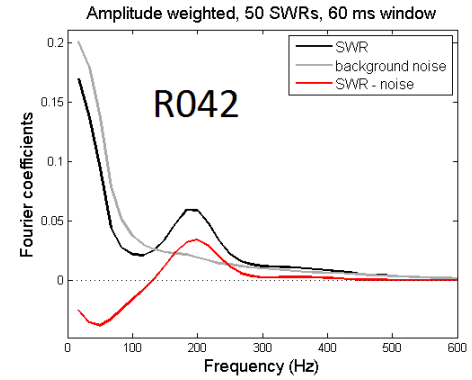

(a)

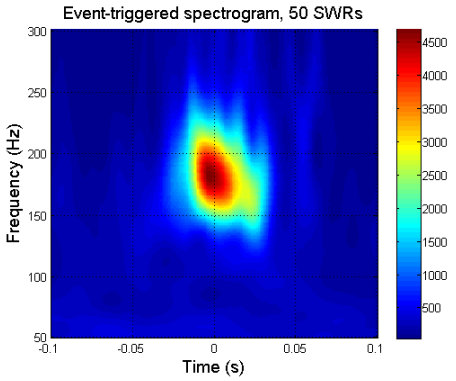

(b)

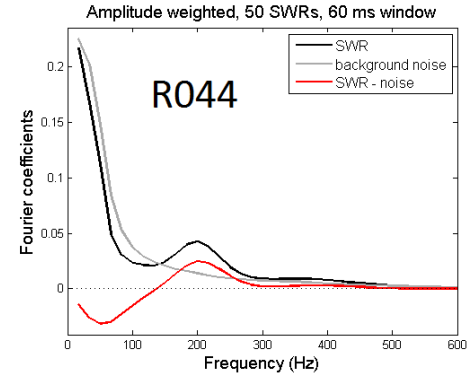

(c)

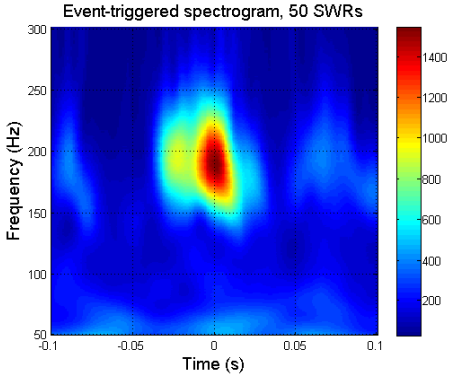

(d)

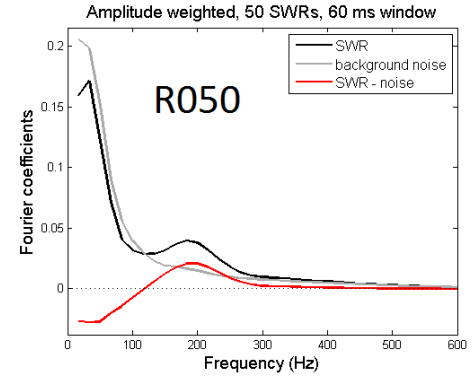

(e)

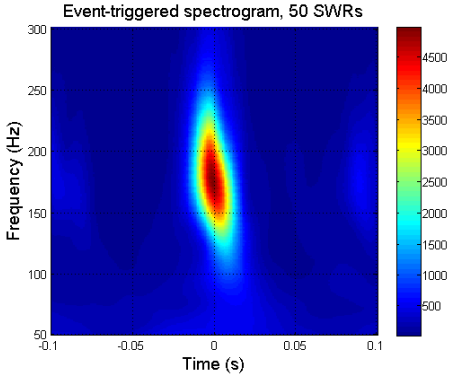

(f)

Figure 4.7: Noise-corrected frequency spectra and event-triggered spectrograms for manually identified SWRs. (a, c, e) Spectra used for detecting SWRs in the LFP. Fourier coefficients for hippocampal background noise are plotted in grey, while Fourier coefficients for manually identified SWRs are plotted in black. The difference between the two sets of Fourier coefficients is plotted in red and comprises the noise-corrected frequency spectrum (NCFS), which describes the relative difference in frequency content between SWRs and background noise. The NCFS displays higher amplitude content between 150–250 Hz. (b, d, f) The corresponding spectrograms for the manually identified SWRs, displaying high power in the frequency band 150–250 Hz typical of rodent SWRs. The time axis ranges $\pm$ 0.1 s around the center of each SWR.

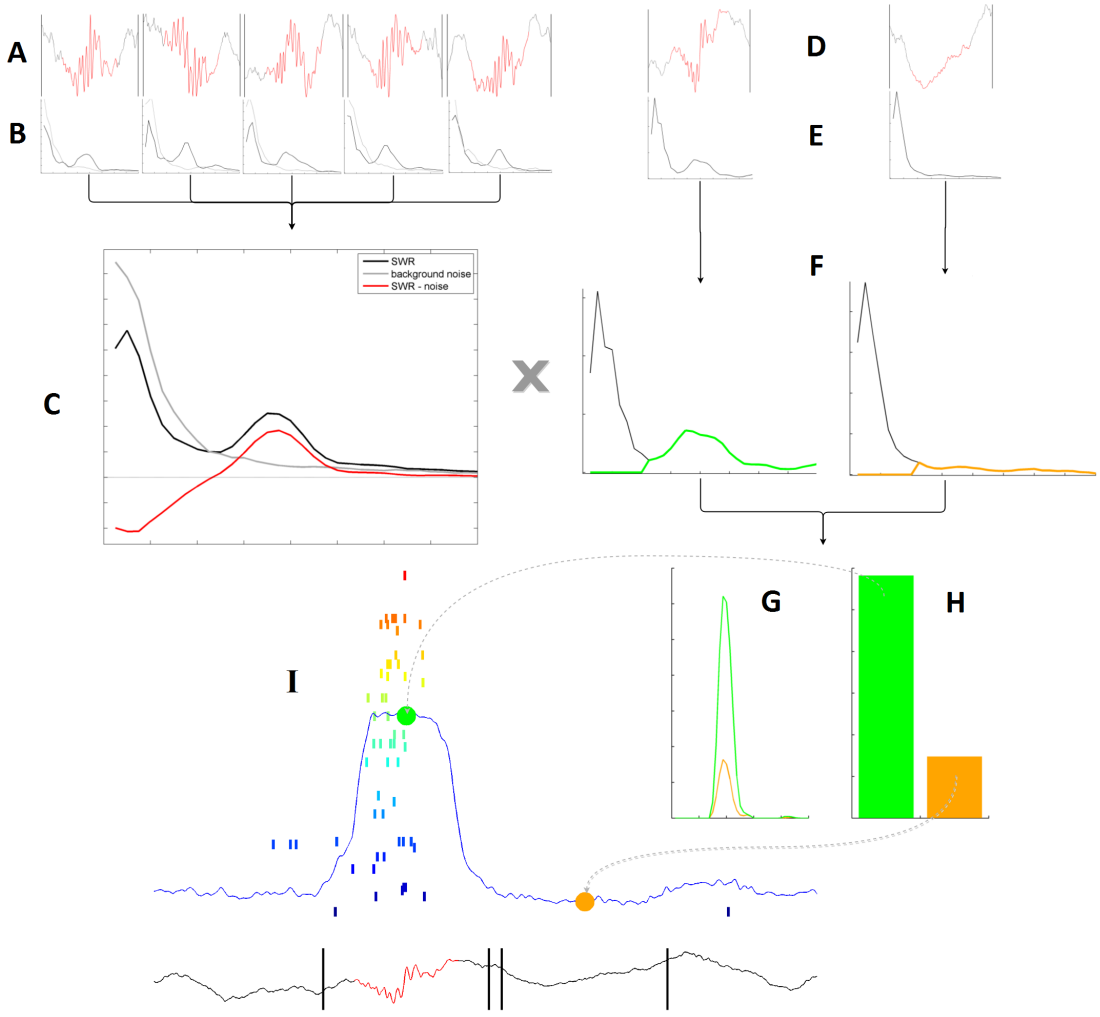

Figure 4.8: Steps in sharp wave-ripple detection. (A) Manually identify SWRs. (B) Obtain the Fourier coefficients for each SWR. (C) The noise-corrected frequency spectrum is obtained from element-wise summation of the Fourier coefficients for hippocampal background noise and SWRs, followed by subtraction of noise from SWRs (gray – Fourier coefficients hippocampal background noise; black – Fourier coefficients SWRs; red – noise-corrected frequency spectrum). (D) The SWR detector changes its viewing window along the LFP and looks at specific segments (an example of a SWR, left, and a non-SWR, right), then it obtains (E) the Fourier coefficients for those segments and removes all frequencies below 100 Hz (F: SWR, left, green; non-SWR, right, orange). Next, (in panel G) it multiplies the Fourier coefficients (from panel F) by the noise-corrected frequency spectrum (red from panel C) and then sums all of the values together to get a single score for the current viewing window (H). The scores for different viewing windows are aggregated into a score vector as the detector moves along the LFP data, blue line in panel (I), with LFP plotted below. Notice that the score for the SWR (green dot) is much higher than the score for the non-SWR (orange dot). Also notice the high degree of neuron spiking activity (colourful tick marks) associated with the SWR.

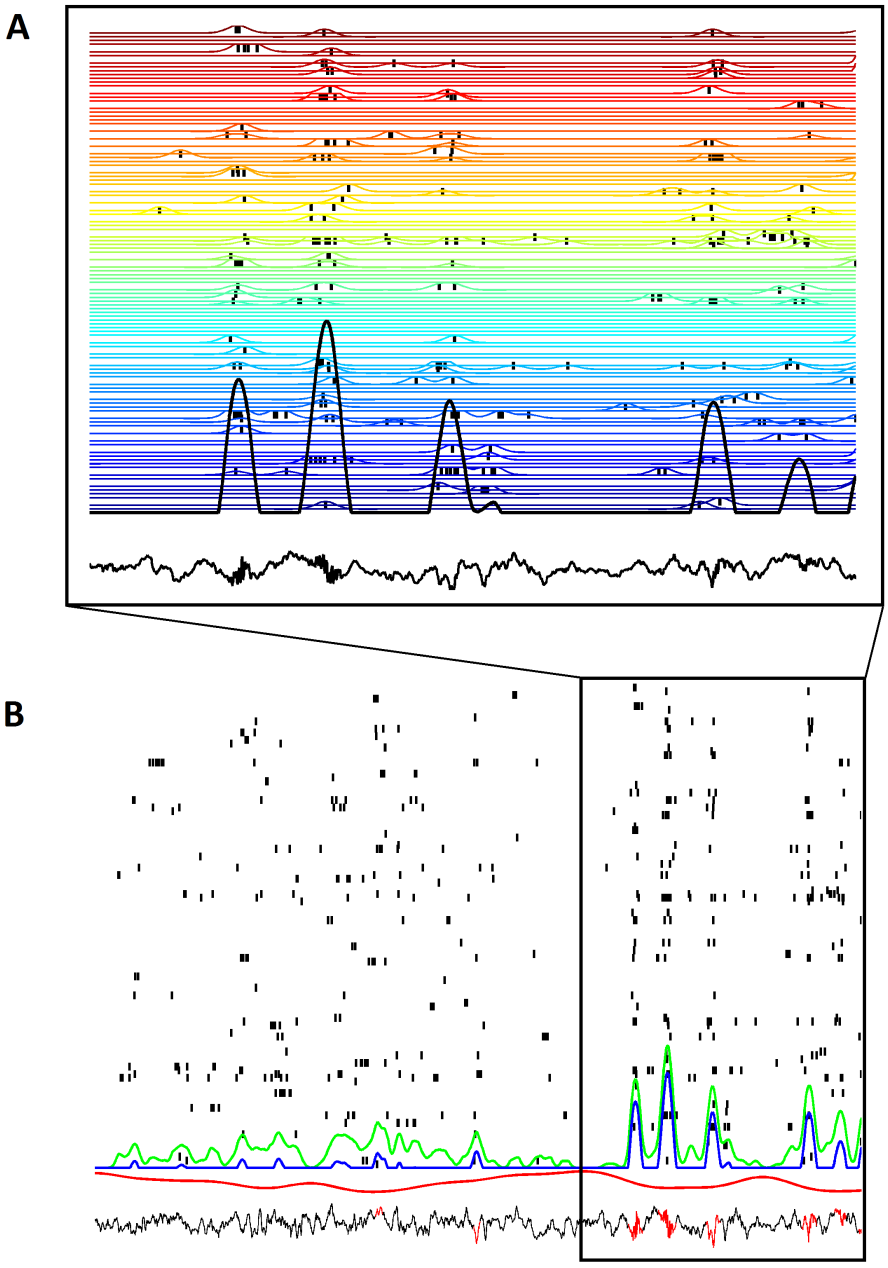

Figure 4.9: Multiunit activity detection. (A) A raster plot with LFP plotted below (viewing window, 1.5 s). Each coloured line represents $s(t)$ the spike contribution from a single cell in the raster plot. The contributions from each cell are summed and undergo adaptive thresholding to produce the final score curve $M(t)$ (black). (B) Shows the raw summed multiunit activity score for all cells together $S(t)$ (green curve), the adaptive thresholding score $A(t)$ (red curve) which is subtractive, and the resulting final multiunit activity score $M(t)$ (blue curve). The local field potential is shown below, with detected events highlighted in red (viewing window, 4 s). Note that the left half of the raster plot is dominated by non-SWR-associated multiunit activity, and more of these regions would have been detected as false positives without adaptive thresholding.

4.2.3 Place Fields

Place field estimation requires spiking data and position data. Since the number of passes the rat makes through the left and right arms is uneven, a subset of the trials for the favoured arm are chosen to match the number of trials for the unfavoured arm. The trial matching is done so that the temporally nearest favoured trial is matched to each unfavoured trial. In doing this we maximize the likelihood that the rat was in a similar behavioural state and that place fields for both arms are estimated based on similar amounts of position data.

Position data is then separated into matched left and right trial times, linearized along the two possible trajectories (so that the rat's position can be described using a single scalar value defined from the start of the track) and binned into 3-cm bins. Likewise, spiking data is also separated into left and right trials, but then restricted to exclude times when the rat's head was moving slower than 4 cm/s. Firing rate maps (or turning curves) are computed by binning spikes in 3-cm bins, dividing by the occupancy, and smoothing with a Gaussian kernel (σ = 3 cm). The locations of place field centers (peak firing rate) are defined with respect to the entry point on the central arm of the track. Cells with fields before the choice point or with fields on both arms are excluded from analysis.

4.2.4 Measuring Ensemble Neural Activity

Once the place fields have been obtained we can see if prospective place cell firing reflects the animal's motivational state. To do this we examine how pairs of cells fire together during HFEs recorded before the rat has been on the track that day (the prerecord), and infer whether this activity likely represents the left (food) or right (water) arms of the track. We use two ways of measuring ensemble neural activity: co-occurrence analysis and sequence analysis. Briefly, co-occurrence analysis looks at the activity of cell pairs during HFEs, whereas sequence analysis looks at the temporal activity of all cells during given HFEs to see if they qualify as replay events.

Co-occurrence analysis

Co-occurrence, or coactivation, analysis allows us to examine the activity of neural populations for behavioural correlations even in cases where there are too few active cells to perform sequence-based analyses. It involves checking if there is coordinated activity, or joint firing probability, between left-only or right-only cell pairs in HFEs that occurs more often than expected by chance.

First, neural units (cells) are classified according to which arm the fields are located on (left or right). Then, spiking data during the prerecord is converted into an nCells $\times$ nHFEs matrix, Q, organized such that each row corresponds to a cell, and each column groups the spikes into 100 ms time bins defined around the centers of the candidate event intervals. Thus, each column contains information about which cells were active together during a given candidate event [13]. From Q we obtain p_0, the fraction of events each cell was active in individually (Equation 4.6). We also obtain p_{obs}, which is the observed co-occurrence (joint firing probability of cell a and cell b), and p_{shuf}, which is the co-occurence expected by chance based on randomly shuffled data (250 shuffles). Each shuffle consists of the following steps: 1. randomly permute the contents of the time bins for each cell in Q to create Q_{perm}; 2. determine the co-occurrences observed in Q_{perm} to obtain Q_{shuf}. Then, the mean co-occurrence across each shuffle in Q_{shuf} is taken to construct p_{shuf}. Finally, to compute the Z-score probability, p_z, we normalize the difference between the observed co-occurrence, p_{obs}, and the randomly shuffled co-occurence, p_{shuf}, by the standard deviation, σ, of the shuffled co-occurrences in Q_{shuf} (Equation 4.7). The null hypothesis is that p_{obs} and p_{shuf} are the same.

$$p_0 = \frac{N_{\text{active}}}{N_{\text{total}}} \tag{4.6}$$

$$p_z(a,b) = \frac{p_{\text{obs}}(a,b) - p_{\text{shuf}}(a,b)}{\sigma(Q_{\text{shuf}})} \tag{4.7}$$

Data from all rats is collected and a two-way analysis of variance (ANOVA) is performed to find the main effects of arm choice and restriction condition, and the interactions between arm choice and restriction condition, on cell pair coactivity.

[13] We exclude pairs of cells recorded on the same tetrode as a precaution against the limitations of spike sorting.

Sequence analysis

Sequence analysis involves looking at what are generally referred to as replays corresponding to previous environmental experiences. It involves checking if place cell activity during HFEs is significantly ordered so as to reflect trajectories on the track. Since there was not enough data to perform sequence analysis (see Results), we will briefly describe the method for identifying significantly ordered sequences and present qualitative results in the Results section.

Unlike co-occurrence analysis, here we order the neural units (cells) according to field location in addition to classifying them as left or right. So, for instance, cells with fields on the left side of the track are placed in one group and ordered so that the cells with fields closest to the choice point are first and cells with fields closest to the reward site are last. The two groups can be thought of as forming raster plots: the y-axis contains the ordered spiketrains of cells and the x-axis is time. Next we apply a NAU threshold based on the new sample of (left-arm- or right-arm-only) cells, so that only the candidate events with 5 or more active arm cells are considered for further analysis. If a session has zero candidate events left after NAU thresholding, the session cannot undergo sequence analysis.

For the remaining sessions, Spearman's rank-order correlation is performed on the spikes within each candidate event to see if the temporal organization of firing reflects spatial organization of place fields on the track (Figure 4.10). At the same time we create two sets of shuffled data (250 shuffles). The first set contains spiketrains that have undergone temporal shuffling: each spike within a candidate event is reassigned a new, random time within the candidate interval (uniform random distribution, so that each combination of spiketimes is equally likely as any other combination). The second set contains spiketrains that have undergone identity shuffling: the spiketrains are given a different random order, equivalent to the cells exchanging place field locations on the track. In both cases, the overall number of spikes within each candidate interval remains the same—the spiketimes are changed in the time shuffling, while the place field locations are changed in the identity shuffling. The rank-order correlation is computed for these two sets of shuffled data;

if the correlations for the observed (real) data is significantly different from those of the shuffled data ($p < 0.01$) we consider the sequence within the candidate event to be significantly ordered, i.e. we consider it to be a replay. Then, we quantify the left and right replays and see if they reflect the rat's restriction condition (motivational state). The null hypothesis is that he replays the left arm and right arm equally on food and water days.

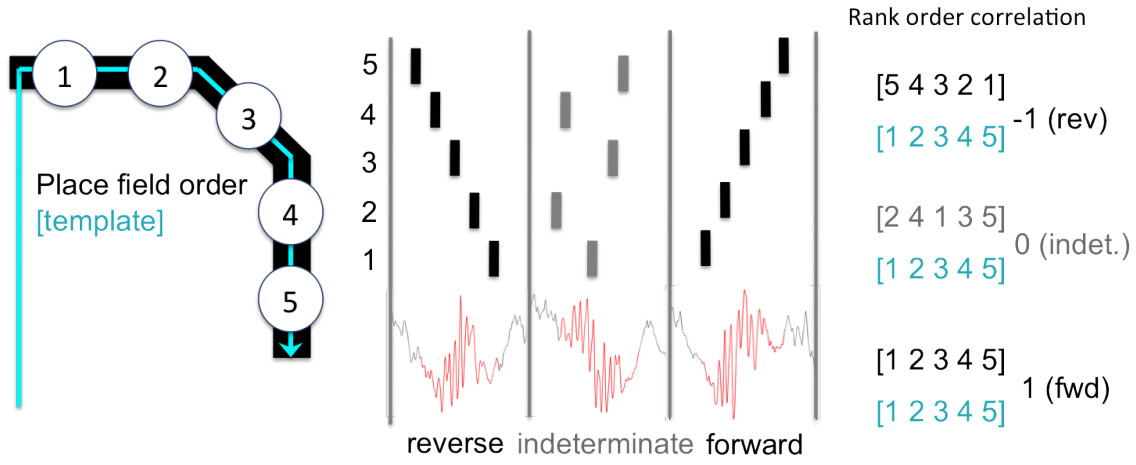

Figure 4.10: Identifying sequences. This example simplifies how we compute rank order correlations. The left panel shows a schematic of the right arm of the T-maze along with place fields that the rat would pass through as he makes his way to the reward. This place field order (1,2,3,4,5) forms the template sequence. The middle panel shows possible spiking orders during three different sharp wave-ripples for the five place fields in the example. The right panel illustrates how we compare the template sequence (cyan) and observed sequence (black, as seen in the middle panel) to get a rank order correlation. Positive correlations are forward replays whereas negative correlations are reverse replays. Rank order correlations are also computed for shuffled data. Essentially, sequences are considered to be significantly ordered if they are very rarely observed in the shuffled data.

5. Results

We recorded from CA1 neurons while three rats performed a motivational shift task so that we can examine whether motivational state influences the content of HFE-associated spiking activity.

5.1 Behaviour

Overall, rats chose to approach reward arms corresponding to their restriction condition (Table **??**, Figure 5.1a). Approach probabilities were calculated based on 18 session from 3 rats. Blocked trials and runback trials[1] were excluded from analysis, leaving a total of 144 trials for food days and a total of 141 trials for water days. On food restriction days rats chose the food arm more often (125/144, p_{food} = 0.87; 19/144, p_{water} = 0.13) and on water restriction days, they chose the water arm more often (112/141, p_{water} = 0.79; 29/141, p_{food} = 0.21). Overall behavioural choices were significantly different from chance for both food ($p < 0.001$) and water($p < 0.001$) restriction days. Considering the choice probability across trials in the average session reveals that choosing the restricted substance on the first trial was approximately random, p_{first} = 0.56 for food and p_{first} = 0.44 for water. The probability of making a correct choice generally increased across the session, suggesting that rats may have been relying on a working memory strategy to remember where to go (Figure 5.1b).

Mean trial latency, or the average amount of time it took for the rat to complete a trial, was also considered for arm choice under restriction condition. Before computing latencies, trials toward the favoured

[1] Blocked trials are any trials where the rat was forced down an experimenter-determined arm; Runback trials are any trials where the rat attempted to reverse directions before choosing an arm.

arm were downsampled to match the number of trials down the unfavoured arm such that the temporally nearest favoured trials to unfavoured trials were chosen. This resulted in 99 food arm trials and 99 water arm trials. On average, rats completed trials more quickly when the restricted arm was approached (Figure 5.2). The mean latency when approaching the food reward and water reward on a food restriction day was 5.1 ($\pm$1.9 SEM) seconds and 17.4 ($\pm$9.3 SEM) seconds respectively; the mean latency when approaching the food reward and water reward on a water restriction day was 11.4 ($\pm$7.1 SEM) seconds and 5.4($\pm$ 1.2 SEM) seconds respectively. Since many of the trials down the unfavoured arm were forced trials, the latency data suggest that rats strongly preferred not to approach the non-restricted reward compared to the restricted reward. Rats would often stop on blocked trials to investigate the barrier, were reluctant to go the blocked route, or would try to reverse directions. A two-way ANOVA performed on mean latency found a significant interaction between approach arm and restriction type ($p < 0.001$), and significant main effects for approach arm ($p < 0.05$) and restriction type ($p = 0.05$). Further evidence that the restriction regime manipulated the rats' motivational states is that upon return to the home cage, rats would consume the restricted substance for extended periods of time, even though the non-restricted substance was freely available at the same time.

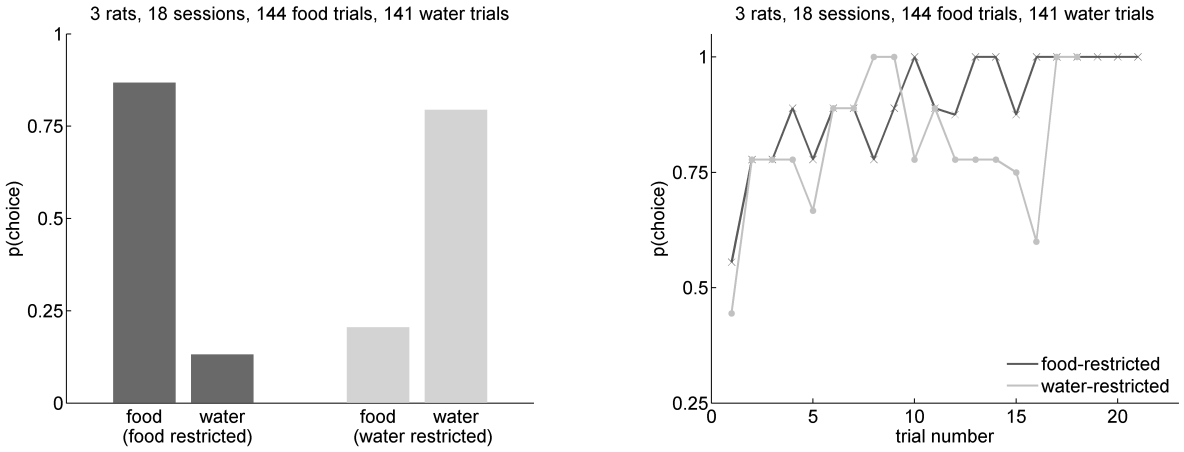

(a) **(b)**

Figure 5.1: Arm choice and restriction condition. (a) Overall reward arm approach probabilities under food restriction and water restriction: food was preferred on food days, while water was preferred on water days. Rats completed a total of 144 trials on food restriction days, with 125 of those being toward the food arm and 19 toward the water arm. They completed 141 trials on water restriction days, with 112 trial toward the water arm and 29 toward the food arm. (b) The probability of choosing the restricted reward across trials: dark grey–the probability of choosing food when food restricted; light grey–the probability of choosing water when water restricted. Note that the probability of choosing the reward that corresponded to restriction state generally increased with trials.

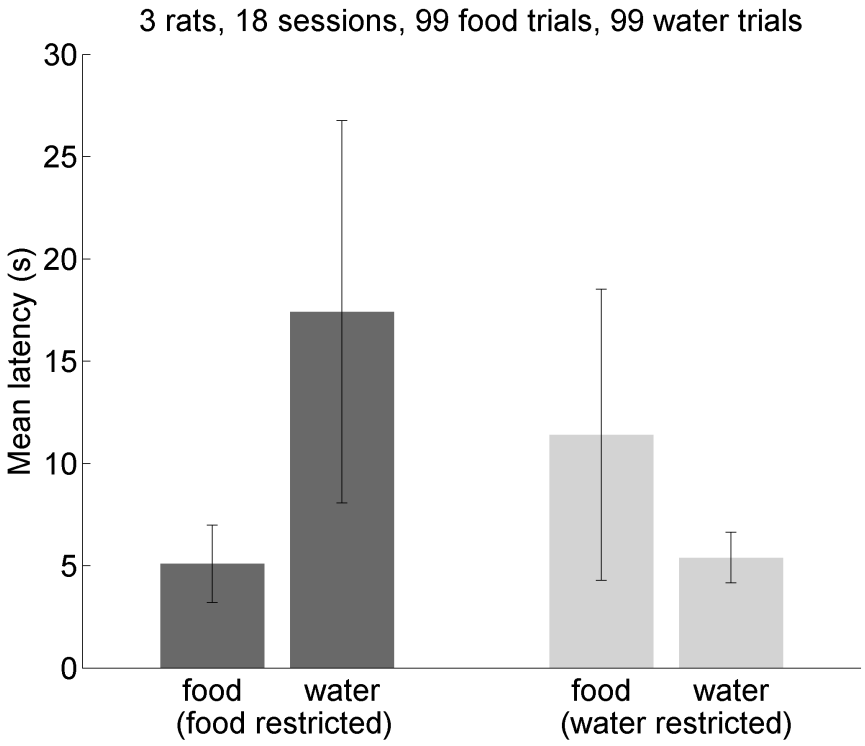

Figure 5.2: Mean trial latency. Rats approach the restricted substance more quickly than they approach the non-restricted substance. Latency data is for matched trials only, and is averaged across all rats and all sessions.

5.2 Neural units

A total of 1,207 neural units[2] were recorded from three rats across 18 sessions. Of these units, 339 (33%) were recorded from R042, 217 (18%) were recorded from R044, and 591 (49%) were recorded from R050. Unit counts for each session can be found in Table 5.1. Notice that the number of units usually increases and then decreases across sessions . This illustrates the tendency for tetrodes to slowly drifting through the layer.

Table 5.1: Total neural units for three rats across each of their six sessions.

Rat ID	Session 1	Session 2	Session 3	Session 4	Session 5	Session 6	Total
R042	22	74	107	64	73	59	**339**
R044	17	13	43	53	50	41	**217**
R050	72	94	72	113	128	112	**591**

Of the 1,207 neural units recorded, 649 or approximately half (54%) had place fields on the track arms. Of these units, 186 (29%) were recorded from R042, 106 (16%) were recorded from R044, and 375 (55%) were recorded from R050. The units were evenly divided between the left and right arms of the track, with 327 having fields on the left arm and 322 having fields on the right arm (examples of left and right place cells can be found in Figure 5.3). Left- and right-arm counts for each session can be found in Table 5.2. Considering the proportion of units with fields on the track arms, the data for individual rats follows a similar trend as the combined data, with 186/339 (55%) of R042's cells having arm fields, 106/217 (49%) for R044, and 357/591 (60%) for R050.

[2] "Neural unit" is a cautious way of saying "neuron" since we cannot know for sure that each cluster of spikes represents all the output from a single neuron.

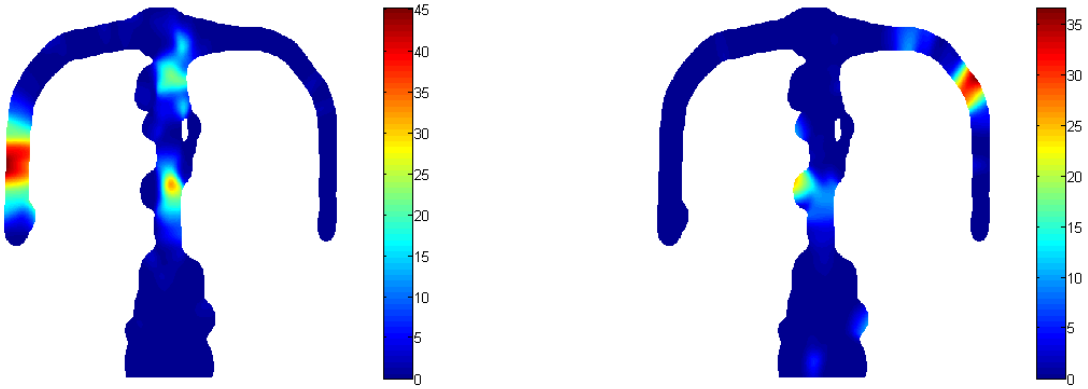

(a) **(b)**

Figure 5.3: Left and right place fields. (a) Place field for a left-arm place cell. (b) Place field for a right-arm place cell. The colourbar indicates firing rate: the cells have higher firing rates in locations where the color is more red, and lower firing rates where the colour is more blue.

Table 5.2: Neural units with fields on the track arms for three rats across each of their six sessions. (L) left arm units; (R) right arm units

	Session 1		**Session 2**		**Session 3**		**Session 4**		**Session 5**		**Session 6**		**Total**
Rat ID	**L**	**R**	**L**	**R**	**L**	**R**	**L**	**R**	**L**	**R**	**L**	**R**	**LR**
R042	4	3	20	12	26	30	13	6	17	16	21	18	**186**
R044	8	8	3	6	12	15	13	9	5	9	6	12	**106**
R050	21	25	32	30	21	27	31	33	40	33	34	30	**357**

5.3 Candidate events

The candidate detection and limiting procedures found a total of 23,890 high-frequency events (HFE) for 16 sessions across 3 rats. Of these events, 9,245 (36.7%) occurred during the prerecord, 6,598 (27.6%) during the task, and 8,047 (33.7%) during the postrecord. Of the HFEs detected during the precord, R042 contributed 2,222 (24%), R044 contributed 1,791 (19.4%), and R050 contributed 5,232 (56.6%). See Table

5.3 for a breakdown of HFEs detected for each segment of the recording session.

Table 5.3: Total candidate events detected for three rats across 18 sessions. The percentages out of the totals are shown in brackets.

Rat ID	Prerecord	Task	Postrecord	Total
R042	2,222 (24.0%)	2,617 (39.7%)	2,584 (32.1%)	7,423 (31.1%)
R044	1,791 (19.4%)	2,292 (34.7%)	1,770 (22.0%)	5,853 (24.5%)
R050	5,232 (56.6%)	1,689 (25.6%)	3,693 (45.9%)	10,614 (44.4%)
All rats	9,245 (36.7%)	6,598 (27.6%)	8,047 (33.7%)	23,890

Time-frequency analysis and spectrograms for average candidates were done using the MATLAB Fieldtrip toolbox (Oostenveld et al., 2011) with frequencies of interest ranging from 1–250 Hz and times of interest $\pm$ 125 ms around the centers of the detected events (Figure 5.4, left column). This was done for a representative session from each rat. Time-frequency analysis with the same parameters was also performed for intervals when the rat was in motion (where HFEs were unlikely to occur) for comparison (Figure 5.4, right column). The purpose of doing this is to verify that the detection procedures were reliably detecting events in the 150-250 Hz range, i.e. HFEs that have similar high frequency content as SWRs[3].

[3]Depending on tetrode positioning in the layer, some SWRs may have high power in low frequencies corresponding to the sharp wave portion rather than the ripple portion.

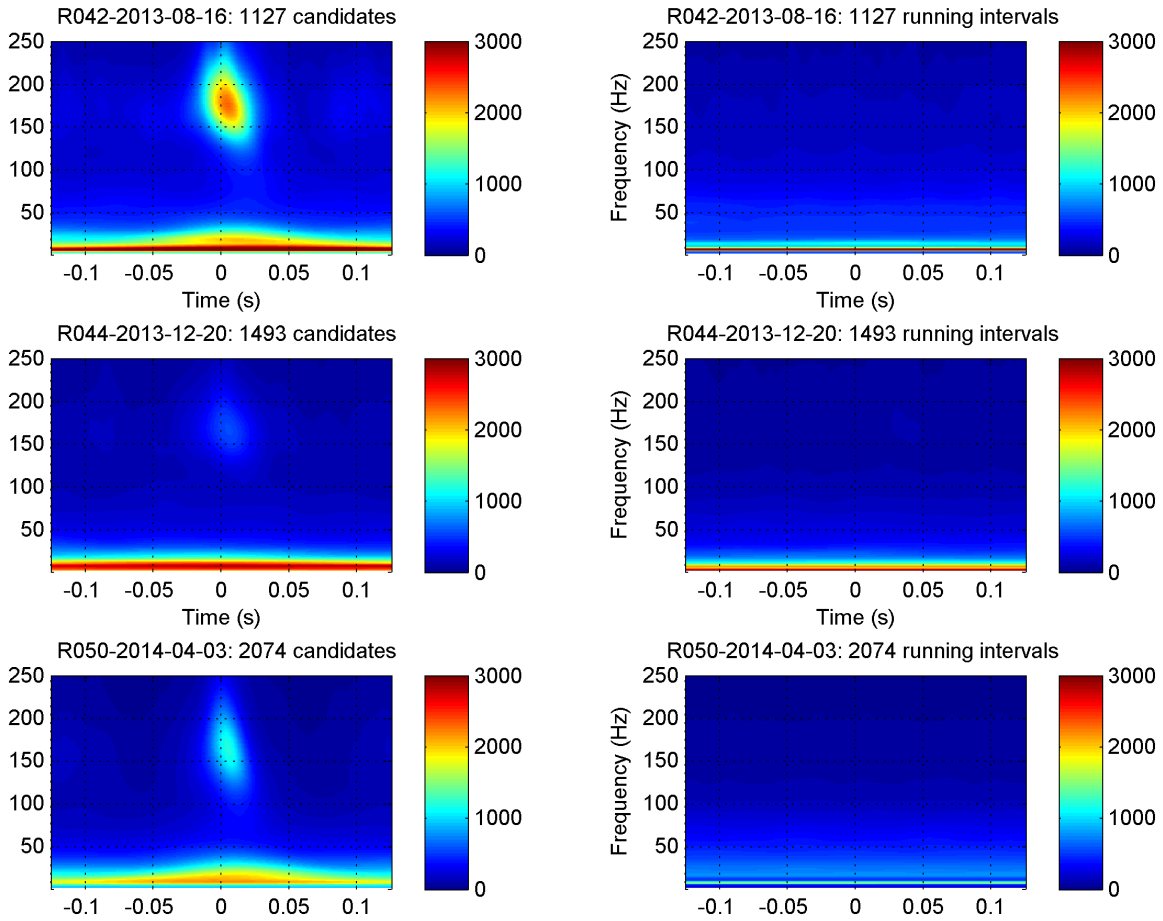

Figure 5.4: Spectrograms for pool of candidate events. Time-frequency analysis was done for candidates from a representative session for each rat. Top row: R042; Middle row: R044; Bottom row: R050. Left column: spectrograms for candidate pool; Right column: spectrograms from running intervals for comparison. The candidate pool has higher power in the frequency band 150–250 Hz compared to the running intervals.

5.4 Co-Occurrence

Considering all food restriction sessions, the mean proportion of HFEs (p_0, Figure 5.5a) that left-arm cells participated in individually was 0.15 ($\pm$ 0.15 SD) and the mean proportion of of HFEs that right-arm cells participated in individually was 0.18 ($\pm$ 0.20 SD). Likewise for water restriction sessions, the mean proportions for left-arm cells and right-arm cells were 0.18 ($\pm$ 0.17 SD) and 0.19 ($\pm$ 0.16) respectively. Overall, cells on the right arm were more likely to participate in HFEs than cells on the left, but this did not interact

with motivational state. Considering Z-score coactivity during HFEs (p_z, Figure 5.5b) for food restriction sessions, for left-only pairs p_z was 0.75 ($\pm$ 2.45 SD) and for right-only pairs it was 0.44 ($\pm$ 2.06 SD). Likewise for water restriction sessions, p_z was 0.68 ($\pm$ 2.35 SD) for left-only pairs and 0.95 ($\pm$ 1.99 SD) for right-only pairs. Overall, Z-score coactivity (co-occurrence) interacted with motivational state ($p < 0.001$). Thus, cell pairs with fields on the food arm were more likely to be coactive during HFEs during food restriction, and and cells pairs with fields on the water arm were more likely to be active during HFEs during water restriction. There was a significant main effect of restriction type on cell pair coactivity (p = 0.01), but not on single cell activity, in HFEs. The field location did not have a significant effect on the overall proportion of candidate events that single cells or cell pairs participated in. See Figures 5.6, 5.7, 5.8 and Table 5.4 for p_0 and p_z values for each rat.

Table 5.4: Individual participation (p_0) and Z-score coactivity (p_z) of place cells in HFEs, p ($\pm$SD). The left arm has a food outcome and the right arm has a water outcome.

	Food restricted				**Water restricted**			
	left arm		**right arm**		**left arm**		**right arm**	
Rat ID	p_0	p_z	p_0	p_z	p_0	p_z	p_0	p_z
R042	0.10 (0.12)	0.45 (1.95)	0.18 (0.26)	0.82 (1.69)	0.19 (0.18)	-0.01 (1.63)	0.11 (0.15)	1.63 (1.50)
R044	0.16 (0.12)	0.34 (1.17)	0.30 (0.32)	0.00 (1.07)	0.23 (0.24)	-0.31 (0.97)	0.24 (0.21)	0.37 (1.58)
R050	0.19 (0.16)	0.97 (2.78)	0.15 (0.14)	0.41 (2.11)	0.15 (0.13)	0.96 (2.53)	0.19 (0.14)	1.02 (2.04)
All rats	0.15 (0.15)	0.75 (2.45)	0.18 (0.20)	0.44 (2.06)	0.18 (0.17)	0.68 (2.35)	0.19 (0.16)	0.95 (1.99)

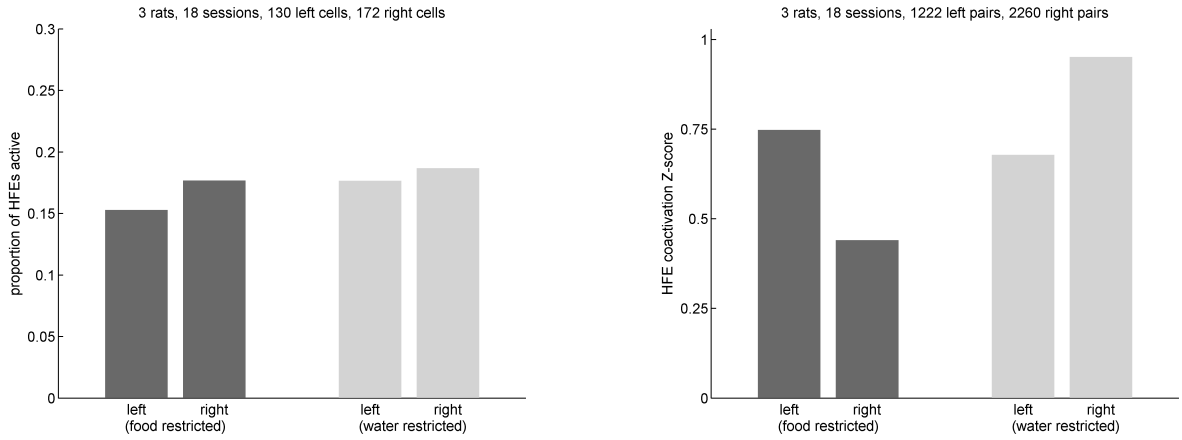

(a) **(b)**

Figure 5.5: Participation and coactivity of place cells in SWRs for all rats. (a) Proportion of SWRs left-only and right-only place cells participated in on food-restriction and water-restriction days (mean p_0 for all rats and all sessions combined). (b) Z-score coactivity of left-only and right-only place cell pairs in SWRs on food-restriction and water-restriction days (mean p_z for all rats and all sessions combined).

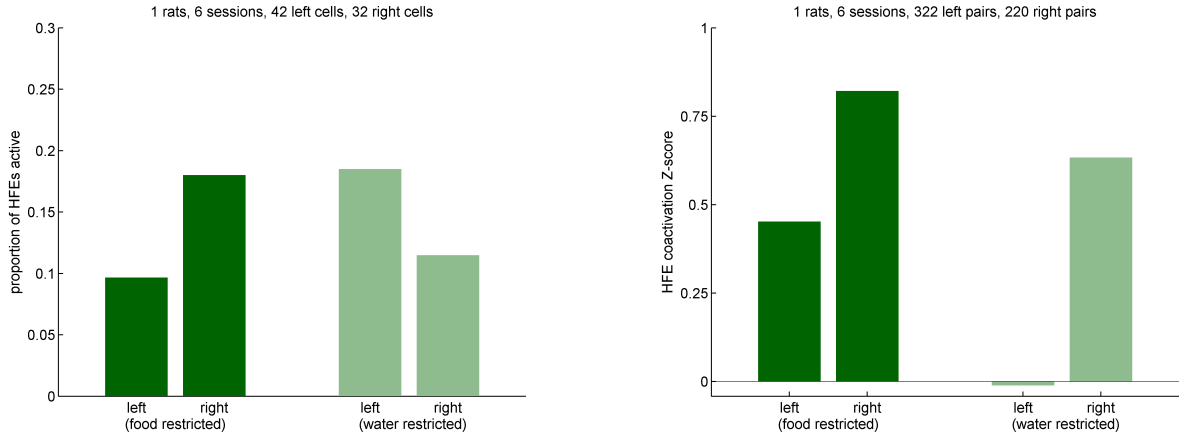

(a) **(b)**

Figure 5.6: Participation and coactivity of place cells in HFEs for R042. (a) Proportion of SWRs left-only and right-only place cells participated in on food-restriction and water-restriction days (mean p_0). (b) Z-score coactivity of left-only and right-only place cell pairs in SWRs on food-restriction and water-restriction days (mean p_z).

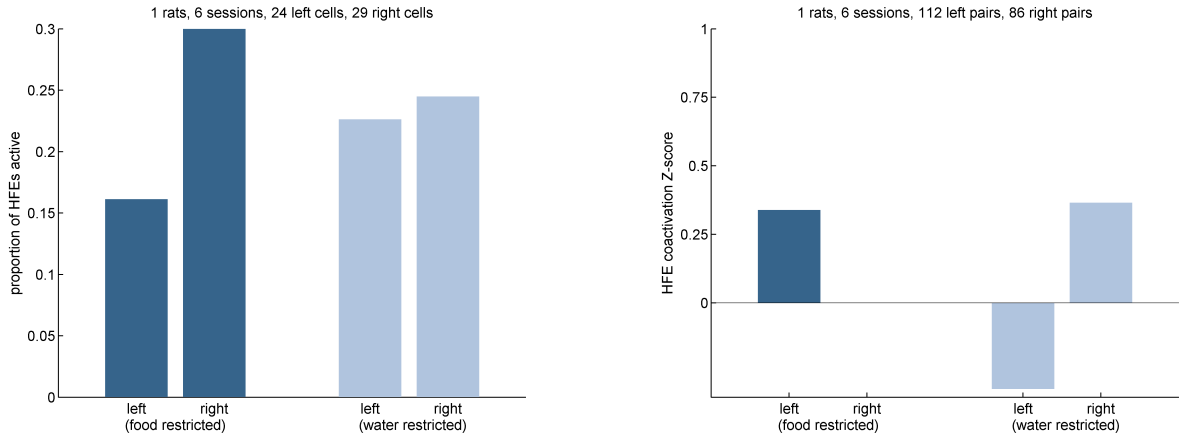

(a) **(b)**

Figure 5.7: Participation and coactivity of place cells in HFEs for R044. (a) Proportion of SWRs left-only and right-only place cells participated in on food-restriction and water-restriction days (mean p_0). (b) Z-score coactivity of left-only and right-only place cell pairs in SWRs on food-restriction and water-restriction days (mean p_z).

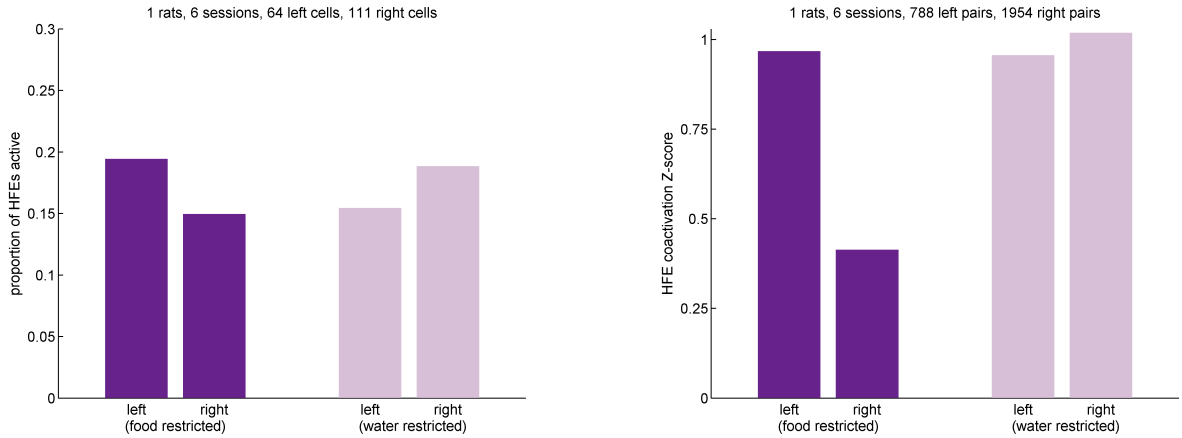

(a) **(b)**

Figure 5.8: Participation and coactivity of place cells in HFEs for R050. (a) Proportion of SWRs left-only and right-only place cells participated in on food-restriction and water-restriction days (mean p_0). (b) Z-score coactivity of left-only and right-only place cell pairs in SWRs on food-restriction and water-restriction days (mean p_z).

5.5 Sequences

Sequence analysis begins with thresholding the candidate pool a second time, in addition to the thresholding during detection. This time the events are limited based on the number of active place cells that have fields located on the track, rather than the total population of recorded place cells. If any sessions belonging had zero candidate events left after NAU thresholding with left-arm and right-arm cells, the session was not able to be used for sequence analysis. This disqualified two sessions from R042 and five sessions for R044. NAU thresholding did not disqualify R050's data from sequence analysis (see Table 5.5 for the number of prerecord candidate events remaining after NAU thresholding).

Table 5.5: Number of prerecord candidate events after NAU thresholding with left-arm and right-arm place cells. (T) total candidate pool; (n) number of events remaining after NAU thresholding

	Session 1		**Session 2**		**Session 3**		**Session 4**		**Session 5**		**Session 6**	
	T	**n**	**T**	**n**	**T**	**n**	**T**	**n**	**T**	**n**	**T**	**n**
R042	342	0	186	4	370	51	402	0	473	35	440	54
R044	292	0	143	0	357	17	451	0	625	0	642	0
R050	710	70	664	220	496	253	814	553	1557	1176	991	812

Sequence detection was performed on all qualifying sessions, however, zero significant sequences were found for R044's single day of data, and only one significant sequence was found for all of R042's data combined. Thus, the results here focus only on R050's data. The number of R050's candidates that contained significantly ordered sequences can be found in Table 5.6.

On food restriction days, R050 produced a total of 17 significant left arm replays and a total of 18 significant right arm replays; on water restriction days, he produced 12 left replays and 24 right replays. An example of a left-arm and right-arm replay can be found in Figure 5.9. Considering the proportion of significant[4] left and right sequences for R050 across six sessions (Figure 5.10), results are signficant for

[4] As mentioned in the Methods section, if a candidate sequence is significantly ordered compared to randomly shuffled data ($p <$

Table 5.6: Number of significant prerecord sequences (nSignificant) for R050. (L) significantly ordered left (food) arm sequences; (R) significantly ordered right (water) arm sequences. The total number of L and R sequences for Food or Water restriction days is shown at the bottom.

	Session 1		**Session 2**		**Session 3**		**Session 4**		**Session 5**		**Session 6**	
Restriction type	**food**		**water**		**food**		**water**		**food**		**water**	
Sequence	**L**	**R**	**L**	**R**	**L**	**R**	**L**	**R**	**L**	**R**	**L**	**R**
nSignificant	0	0	0	0	1	3	6	5	16	15	6	19

water days only ($p < 0.05$)[5]. In other words, R050 was producing prospective replays of the water arm when he was water restricted, and we can reject the null hypothesis that he replays the food and water arms equally. Looking at each day individually, the one day with significant results is the sixth and final session with 6 food arm prospective replays and 19 water arm prospective replays ($p < 0.01$). Without this day, the results are not significant. However, there is an important problem with the restriction regime on this day in particular: an animal care technician erroneously gave him access to water for 30 minutes before the session began. It is worth noting that R050 may have still be water-motivated on this day since his behaviour on the task was in line with his planned restriction condition: he freely chose the water arm 15 times and the food arm once. Furthermore, upon return to the home cage he consumed plain water for more than minute before moving onto the food that was available simultaneously. Still, this does not rule out that the sucrose water available to him during the task may be considered a treat (as chocolate might) rather than a substance the rat views solely as a means for quenching thirst.

0.01), then the sequence is considered to be a replay.

[5]In other words, the odds of flipping a coin 12+24 times on a water day and having it come up as 12 food and 24 water is 0.05, meaning we can reject the null hypothesis that the coin flips are equal.

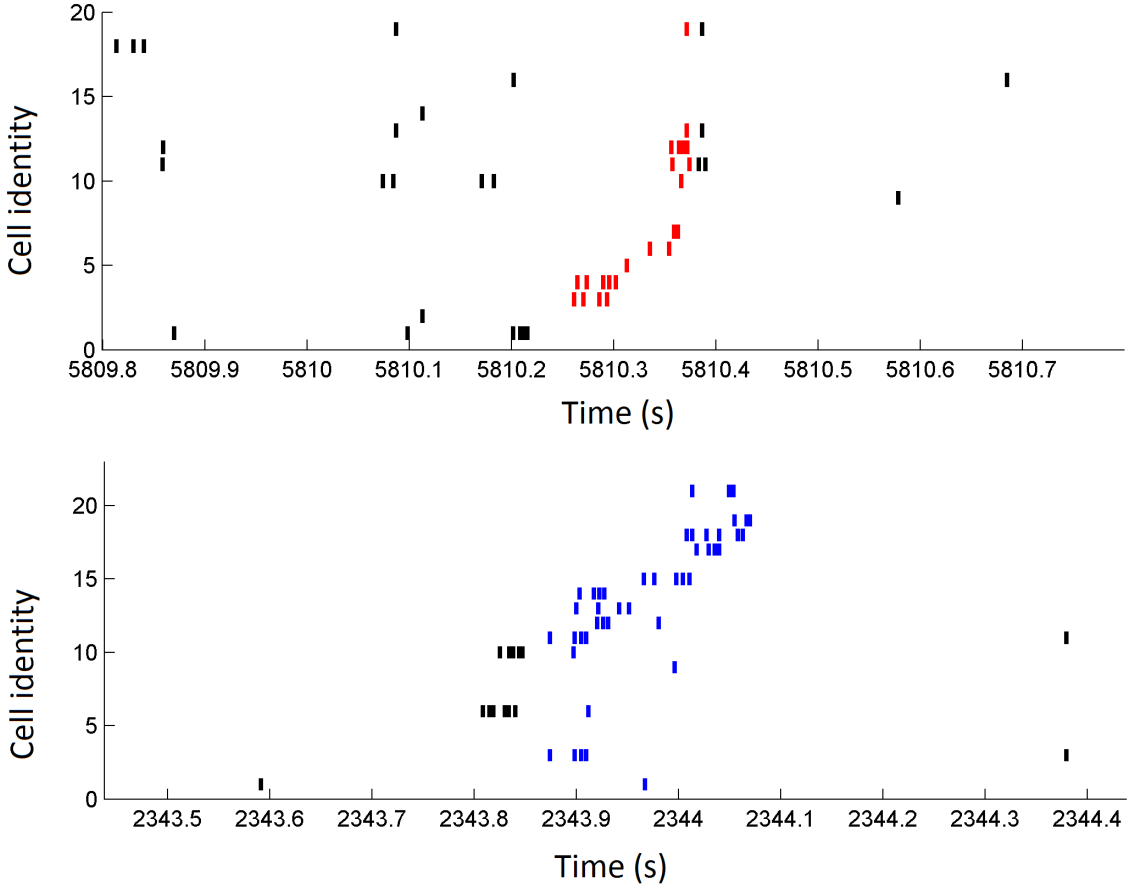

Figure 5.9: A raster plot of a food arm and water arm replay from R050's sixth session. (Upper panel) A significant sequence representing a food (left) arm replay with 10 active neural units. (Lower panel) A water (right) arm replay occurring at a different time with 14 active units. Cells are numbered so that those with place fields closer to the reward site appear at the top. Coloured spikes are contained within the boundaries of the detected events, but it is clear that some of the sequence activity belonging to the events is beyond the detection boundary. Both events were recorded during the prerecord, and are between 100-200 ms in duration.

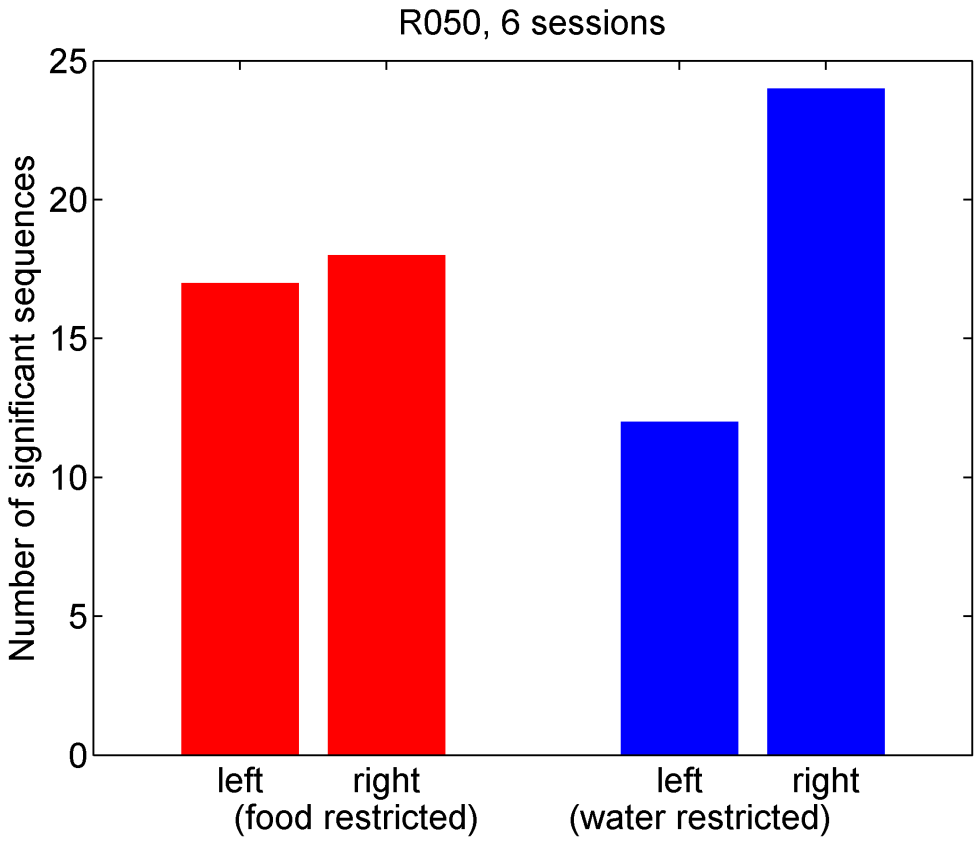

Figure 5.10: Significantly ordered sequences for R050 across three food restriction sessions and three water restriction sessions. For food restriction days, there are a total of 17 left (food) arm replays and 18 right (water) arm replays. For food restriction days, there are a total of 12 left (food) arm replays and 24 right (water) arm replays. The results are significant for water days only ($p < 0.05$).

6. Discussion

We have demonstrated that motivational states influence the content of prospective place cell representations prior to a motivational shift task. We used both 1. Co-occurrence analysis to determine if cell pair coactivity during HFEs reflected motivational state, and 2. Sequence analysis to determine if rats replay motivationally-relevant trajectories more often than expected by chance. To our knowledge, this is the first study that has considered whether motivational states influence the content of prospective non-local hippocampal sequences.

Overall, co-occurrence results suggest that food-restricted rats are more likely to represent the food arm, whereas water-restricted rats are more likely to represent the water arm. This was apparent when the coactivation probably of food-arm cells on food restriction days was greater than would be expected based on chance, and vice versa for water-arm cells. Not only was there a significant interaction between place field location and restriction condition, but there was also a significant main effect of restriction condition on cell pair coactivity. In other words, motivational state influenced the proportion of HFEs that motivationally-relevant trajectory cell pairs participated in. Considering the co-occurrence data for individual rats, however, there was not an observable pattern. R042 represented the water arm more often under both food and water restriction. R044, who had the smallest sample of neural units, represented the reward arm corresponding to his restriction condition. Finally, R050—though his results are also in line with his motivational state—represented the food arm notably more on food days, but this large difference was not present for the water arm on water restriction days, even though water-arm cell pairs were only slightly more likely to co-occur than food-arm cell pairs. This does not agree with the sequence-based results for R050, which found that the right arm was slightly more represented on food restriction days, while the right arm was significantly more

represented on water days.

Although sequence-based results were limited mainly to a single day (session 6) from R050, the results are promising: a thirst-motivated rat replayed water arm trajectories significantly more often than expected by chance. However, given that these conclusions are mainly derived from a single day of data, it raises the question of why the other sessions did not display similar results. This may be due to multiple factors not limited to the requirement for large place cell populations in order to perform sequence-based analyses. Firstly, based on the fact that the first choice was not reliably the restricted substance, and performance generally increased in subsequent trials, rats may have been relying on a working memory strategy to find the rewards. The fact that the final recording day had significant replays may signify the first day R050 was able to evaluate the possible choices and decide on the correct goal arm prior to resampling the environment.

Another possibility is that R050 has a preference for sucrose water, and thus always recalls the water arm when he is present in the room where this reward is available. On food days, such as session 5, he then also replays a greater number of food trajectories reflecting his current restriction condition, while still displaying his preference for sucrose water as a treat. Yet another possibility is that this reflects evolutionary ecology. Consider a rat's natural environment. A rat may be able to forage randomly and easily acquire enough food for its energy demands. If a rat requires water that it cannot obtain from its food source, then it probably needs to navigate to a known water source since water is not typically scattered in the environment. So if this is the case, it could be that the rat brain did not need to evolve mechanisms that plan trajectories for food acquisition many minutes in advance, whereas it did for water acquisition. We already know from previous studies (Singer et al., 2013; Pfeiffer and Foster, 2013) that food motivated rats represent future trajectories that are temporally close to the rat's current context, but these tasks recorded neural activity produced immediately before upcoming behaviour and may reflect the rat's current decision-making process.

How can we be certain that the food and water restriction regimes were successful; i.e. how can we tell if the rat's motivational state is the same as his restriction condition? A rat's overall behavioural choices were in line with the restriction: he chose to approach the restricted substance significantly more

often than he would if choosing randomly. Furthermore, the longer latency for the non-restricted arm on blocked trials suggests he was not interested in approaching this reward, even when no other options were available. However, the longer latency may also result from a rat's natural tendency to investigate novel items (Ameen-Ali et al., 2015): the barrier was not present before, and it is blocking the desired route. Regardless of the rat's interactions with the barrier, the slower latency may still point out that the rat was less interested in immediately approaching the non-restricted reward than he was in investigating the barrier. A final piece of evidence that the restriction regime was successful is that rats consumed the restricted substance for extended periods upon return to the home cage, despite the presence of the non-restricted substance.

Idiosyncrasies seen in correct arm choice on the first trial, therefore, may have been due to under-training: i.e. the rat had not learned how to navigate to the reward locations well enough. The fact that the first choice was not reliably the restricted substance raises concerns over the pre-task reactivation results. How can the rat represent trajectories toward a motivationally relevant goal when he apparently does not know where the reward is located? Perhaps he is able to incite fragments of memory traces from prior experience, but is not able to recall the exact paths needed to reach the goals. In this way, he could activate, for example, food-arm place cells without knowing how his current location connects to his goal location in space. This may perhaps be similar to a human who has vivid recollections of streets and restaurants in Boston, but does not remember how to get to Boston from Toronto. It is likely that for the behaviour to align perfectly with restriction condition (all free choices toward the restricted substance) the rats would need to be trained until they reliably chose correctly. However there are concerns that the rat may switch from a hippocampus-dependent navigation strategy to a procedural striatum-dependent automatic strategy.

It may be that a reminder exposure to the track is required to get the rat thinking about the food and water reward locations. A 25-minute wait may feel like an indeterminate amount of time to a rat. This is further extended by the variable amount of time the rat sits on a waiting platform, before recording begins, while the experimenter is adjusting recording parameters in the system. Rats might not directly link sitting on the platform with a future on the track where food and water options are available.

Karlsson and Frank (2009) noted that awake replays had higher fidelity than sleep replays, so if

our sequence detection methods were too stringent and failed to classify low-fidelity replays, then we have been overly cautious. It is worth noting further that rats probably have little control over what place cells are doing during periods of sleep, and they often spent a great deal of time sleeping during the precording period so this fact may have contributed to fewer prospective replays being observed.

How are motivationally-relevant inputs relayed to the hippocampus? It appears to be unknown whether CA1 receives direct projections from centers that detect or signal hunger and thirst centers in the hypothalamus (lateral nucleus, dorsomedial nucleus, ventromedial nucleus). Another likely source is the medial prefrontal cortex (mPFC) which supports decision-making, goal-directed behaviour, and working memory. Inputs pertaining to motivationally relevant goals may arrive at the hippocampus from the mPFC via the nucleus reuniens of the thalamus which is common pathway for both structures (Griffin, 2015). In fact, in evolutionary history, most sensory inputs to the hippocampal formation arrived via the thalamus rather than via the entorhinal cortex, as seen in mammals today (Striedter, 2005), so it would not be implausible that this connection remains important for relaying motivationally relevant information. The importance of coordination within this pathway was confirmed earlier this year, when neural activity in all three structures was prospectively related to the trajectory an animal was taking, suggesting that contextual cues are generated outside of the hippcampus and relayed through a larger circuit involving the medial prefrontal cortex, the nucleus reuniens, and the hippocampus (Ito et al., 2015).

As found in previous work, the content of replay may contain future trajectories (Pfeiffer and Foster, 2013), non recent trajectories (Gupta et al., 2010; Karlsson and Frank, 2009), and even novel trajectories (Gupta et al., 2010). The work presented here adds to a growing body of research that has found additional, non-consolidation processes supported by hippocampal replay events. The last experience the rat had on the track was at least 20 hours prior to the prerecord and most laps were performed on the opposite arm. Place cell activity was related to the current day's motivational state, in that HFE-associated representations were reflective of the arm containing the restricted substance. This substantiates claims made by previous research that the content of some awake replays may be related to retrieval (Jadhav et al., 2012) or planning (Pfeiffer and Foster, 2013; Singer et al., 2013). Here we found that although such prospective full-fledged replays were rare among the total HFE-associated events recorded, their content was significantly affected

by motivational state.

Qualitatively, the rats were often observed pausing at the choice point in early training and during recording sessions, seemingly considering the outcomes of each choice. In previous research (Johnson and Redish, 2007) this behaviour, known as vicarious trial and error—imagining the results of alternate futures depending on one's imminent decision—was accompanied by non-local theta-associated hippocampal sequences. As rats paused at the choice point, the content of theta sequences alternated between two possible routes routes the animal could take. These theta-associated prospective sequences were called forward sweeps. Future analyses involving this data set might consider whether the content of theta sequences is affected by motivational state. It may be that rats more often make goal-motivated decisions on the fly, as they are foraging and navigating their environment, rather than early on when they are segregated from the environment for—in the rat's perspective—an indeterminate amount of time.

In addition to investigating the influence of motivational state on theta sequences, future directions may also include expanding into other internal states. Perhaps we unequivocally find that appetitive motivational states affect hippocampal sequences. What about other internally generated stimuli? Maybe the memory demand on the hippocampus is what affects the content of replay, whether this demand is caused by a need to find motivationally relevant substances (food or water) or any other behaviour a rat may need to do in order to maintain homeostasis. A motivational shift temperature T-maze is fathomable, wherein the rat is manipulated into favouring warm or cool outcomes. It might be that any stimulus that requires a rat to retrieve memory traces for planning incites hippocampal activity. In this case, it may be more appropriate to conclude that the need to plan motivationally-relevant future trajectories based on past experience affects the content of replay.

In conclusion, hippocampal reactivation processes and their function may be more complex than initially understood, being not limited to consolidation processes or reiterations of recent experience. Given that we found a relationship between HFE-associated spiking activity and motivational state, these neural events may be important for mediating retrieval of past behavioural episodes to facilitate planning for motivationally relevant outcomes.

References

Amaral, D. and Lavenex, P. (2007). Hippocampal Neuroanatomy. In Andersen, P., Morris, R., Amaral, D., Bliss, T., and O'Keefe, J., editors, *The Hippocampus Book*, chapter 3. Oxford University Press, New York, New York.

Ameen-Ali, K. E., Easton, A., and Eacott, M. J. (2015). Moving beyond standard procedures to assess spontaneous recognition memory. *Neuroscience and Behavioral Reviews*, 53:37–51.

Balleine, B. W. and Dickinson, A. (1998). Goal-directed instrumental action: contingency and incentive learning and their cortical substrates. *Neuropharmacology*, 37:407–419.

Born, J. and Wilhelm, I. (2012). System consolidation of memory during sleep. *Psychological Research*, 76(2):192–203.

Buhry, L., Azizi, A. H., and Cheng, S. (2011). Reactivation, Replay and Preplay: How It Might All Fit Together. *Neural Plasticity*, 2011:203462.

Buzsaki, G. (1986). Hippocampal Sharp Waves: Their Origin and Significance. *Brain Research*, 398(2):242–252.

Cheng, S. and Frank, L. M. (2008). New Experiences Enhance Coordinated Neural Activity in the Hippocampus. *Neuron*, 57(2):303–313.

Csicsvari, J., Hirase, H., Mamiya, A., and Buzsaki, G. (2000). Ensemble Patterns of Hippocampal CA1–CA3 Neurons during Sharp Wave-Associated Population Events. *Neuron*, 28(2):585–594.

Davidson, T. J., Kloosterman, F., and Wilson, M. A. (2009). Hippocampal Replay of Extended Experience. *Neuron*, 63(4):497–507.

Diba, K. and Buzsaki, G. (2007). Forward and reverse hippocampal place-cell sequences during ripples. *Nature neuroscience*, 10(10):1241–1242.

Dudai, Y. (2004). The Neurobiology of Consolidations, Or, How Stable is the Engram? *Annual Review of Psychology*, 55:51–86.

Dupret, D., O'Neil, J., Pleydell-Bouverie, B., and Csicsvari, J. (2010). The reorganization and reactivation of hippocampal maps predict spatial memory performance. *Nature Neuroscience*, 13(8):995–1002.

Eichenbaum, H. (2014). Time cells in the hippocampus: a new dimension for mapping memories. *Nature Reviews Neuroscience*, 15:732–744.

Eichenbaum, H. and Cohen, N. J. (2014). Can We Reconcile the Declarative Memory and Spatial Navigation Views on Hippocampal Function? *Neuron*, 84(4):764–770.

Eichenbaum, H., Dudchenko, P., Wood, E., Shapiro, M., and Tanila, H. (1999). The Hippocampus, Memory, and Place Cells: Is It Spatial Memory or a Memory Space? *Neuron*, 23(2):209–226.

Euston, D. R., Tatsuno, M., and McNaughton, B. L. (2007). Fast-Forward Playback of Recent Memory Sequences in Prefrontal Cortex During Sleep. *Science*, 318(5853):1147–1150.

Farovik, A., Dupont, L. M., and Eichenbaum, H. (2010). Distinct roles for dorsal ca3 and ca1 in memory for sequential nonspatial events. *Learning and Memory*, 17(1):12–17.

Ferbinteanu, J. and Shapiro, M. L. (2003). Prospective and retrospective memory coding in the hippocampus. *Neuron*, 40:1227–1239.

Ferbinteau, J., Shirvalkar, P., and Shapiro, M. L. (2011). Memory modulates journey-dependent coding in the rat hippocampus. *The Journal of Neuroscience*, 35(25):9135–9146.

Foster, D. and Wilson, M. (2006). Reverse replay of behavioral sequences in hippocampal place cells during the awake state. *Nature*, 440(7084):680–683.

Frankland, P. W. and Bontempi, B. (2005). The organization of recent and remote memories. *Nature Reviews Neuroscience*, 6(2):119–130.

Griffin, A. L. (2015). Role of the thalamic nucleus reuniens in mediating interactions between the hippocampus and medial prefrontal cortex during spatial working memory. *Frontiers in Systems Neuroscience*, 9(29):1–8.

Gupta, A. S., van der Meer, M. A., Touretsky, D. S., and Redish, A. D. (2010). Hippocampal replay is not a simple function of experience. *Neuron*, 65:695–705.

Hayman, R., Verriotis, M. A., Jovalekic, A., Fenton, A. A., and Jeffery, K. J. (2011). Anisotropic encoding of three-dimensional space by place cells and grid cells. *Nature Neuroscience*, 14:1182–1188.

Hollup, S. A., Molden, S., Donnett, J. G., Moser, M. B., and Moser, E. I. (2011). Accumulation of Hippocampal Place Fields at the Goal Location in an Annular Watermaze Task. *The Journal of Neuroscience*, 21(5):1635–1644.

Ito, H. T., Zhang, S.-J., Witter, M. P., Moser, E. I., and Moser, M.-B. (2015). A prefrontal-thalamo-hippocampal circuit for goal-directed spatial navigation. *Nature*, 522:50–55.

Jadhav, S., Kemere, C., German, P. W., and Frank, L. M. (2012). Awake Hippocampal Sharp Waves Support Spatial Memory. *Science*, 336:1454–1458.

Johnson, A. and Redish, A. D. (2007). Neural Ensembles in CA3 Transiently Encode Paths Forward of the Animal at a Decision Point. *The Journal of Neuroscience*, 27(45):12176–12189.

Karlsson, M. P. and Frank, L. M. (2009). Awake replay of remote experiences in the hippocampus. *Nature Neuroscience*, 12(7):913–918.

Kennedy, P. J. and Shapiro, M. L. (2004). Retrieving Memories via Internal Context Requires the Hippocampus. *The Journal of Neuroscience*, 24(31):6979–6985.

Kennedy, P. J. and Shapiro, M. L. (2009). Motivational states activate distinct hippocampal representations to guide goal-directed behaviors. *Proceedings of the National Academy of Sciences of the United States of America*, 106(26):10805–10810.

Larkin, M. C., Lykken, C., Tye, L. D., Wickelgren, J. G., and Frank, L. M. (2014). Hippocampal output area CA1 broadcasts a generalized novelty signal during an object-place recognition task. *Hippocampus*, 24(7):773–783.

Lee, A. K. and McNaughton, B. L. (2002). Memory of Sequential Experience in the Hippocampus during Slow Wave Sleep. *Neuron*, 36(6):1183–1194.

Louie, K. and McNaughton, B. L. (2001). Temporally structured replay of awake hippocampal ensemble activity during rapid eye movement sleep. *Neuron*, 29(1):145–156.

MacDonald, C. J., Lepage, K. Q., Eden, U. T., and Eichenbaum, H. (2011). Hippocampal Time Cells Bridge the Gap in Memory for Discontiguous Events. *Neuron*, 71(4):737–749.

Moita, M. A. P., Rosis, S., Zhou, Y., LeDoux, J. E., and Blair, H. T. (2003). Hippocampal Place Cells Acquire Location-Specific Responses to the Conditioned Stimulus during Auditory Fear Conditioning. *Neuron*, 37:485–497.

Moita, M. A. P., Rosis, S., Zhou, Y., LeDoux, J. E., and Blair, H. T. (2004). Putting Fear in Tts Place: Remapping of Hippoampal Place Cells during Fear Conditioning. *The Journal of Neuroscience*, 24(31):7015–7023.

Moser, E. I., Kropff, E., and Moser, M. (2008). Place cells, grid cells, and the brain's spatial representation system. *Annual Review of Neuroscience*, 39:69–89.

O'Keefe, J. (2007). Hippocampal Neurophysiology in the Behaving Animal. In Andersen, P., Morris, R., Amaral, D., Bliss, T., and O'Keefe, J., editors, *The Hippocampus Book*, chapter 11. Oxford University Press, New York, New York.

O'Keefe, J. and Dostrovsky, J. (1971). The hippocampus as a spatial map. Preliminary evidence from unit activity in the freely-moving rat. *Brain Research*, 34(1):171–175.

O'Keefe, J. and Nadel, L. (1978). *The Hippocampus as a Cognitive Map*. Oxford University Press.

Oostenveld, R., Fries, P., Maris, E., and Schoffelen, J.-M. (2011). Fieldtrip: Open Source Software for Advanced Analysis of MEG, EEG, and Invasive Electrophysiological Data. *Computational Intelligence and Neuroscience*, 2011(156869).

Pavlides, C. and Winson, J. (1989). Influence of Hippocampal Place Cells Firing in the Awake State on the Activity of These Cells During Subsequenct Sleep Episodes. *The Journal of Neuroscience*, 9(8):2907–2918.

Pezzulo, G., van der Meer, M. A. A., Lansink, C. S., and Pennartz, C. M. A. (2014). Internally generated sequences in learning and executing goal-directed behavior. *Trends in Cognitive Sciences*, 18(12):647–657.

Pfeiffer, B. E. and Foster, D. J. (2013). Hippocampal place cell sequence depict future paths to remembered goals. *Nature*, 497:74–81.

Qin, Y.-L., McNaughton, B. L., Skaggs, W. E., and Barnes, C. A. (1997). Memory reprocessing in corticocortical and hippocampocortical neuronal ensembles. *Philosophical transactions of the Royal Society of London. Series B, Biological Sciences*, 352(1360):1525–1533.

Ranck, Jr., J. B. (1973). Studies on Single Neurons in Dorsal Hippocampal Formation and Septum un Unrestrained Rats. *Experimental Neurology*, 41(2):461–531.

Scoville, W. B. and Milner, B. (1957). Loss of recent memory after bilateral hippocampal lesions. *The Journal of Neurology, Neurosurgery, and Psychiatry*, 20(1):11–21.

Shapiro, M. L., Tanila, H., and Eichenbaum, H. (1997). Cues That Hippocampal Place Cells Encode: Dynamic and Hierarchical Representation of Local and Distal Stimuli. *Hippocampus*, 7:624–642.

Singer, A. C., Carr, M. F., Karlsson, M. P., and Frank, L. M. (2013). Hippocampal SWR Activity Predicts Correct Decisions during the Initial Learning of an Alternation Task. *Neuron*, 77(6):1163–1173.

Singer, A. C. and Frank, L. M. (2009). Rewarded Outcomes Enhance Reactivation of Experience in the Hippocampus. *Neuron*, 64(6):910–21.

Skaggs, W. E. and McNaughton, B. L. (1996). Replay pf Neuronal Firing Sequences in Rat Hippocampus During Sleep Following Spatial Experience. *Science*, 271(5257):1870–1873.

Spruston, N. and McBain, C. (2007). Structural and Functional Propoerties of Hippocampal Neurons. In Andersen, P., Morris, R., Amaral, D., Bliss, T., and O'Keefe, J., editors, *The Hippocampus Book*, chapter 5. Oxford University Press, New York, New York.

Striedter, G. F. (2005). *Principles of Brain Evolution*. Sinauer Associates, Inc., Sutherland, Massachusettes.

Tse, D., Langston, R. F., Kakeyama, M., Bethus, I., Spooner, P. A., Wood, E. R., Witter, M. P., and Morris, R. G. M. (2007). Schemas and Memory Consolidation. *Science*, 316(5821):76–82.

Wilson, M. A. and McNaughton, B. L. (1994). Reactivation of Hippocampal Ensemble Memories During Sleep. *Science*, 265(5172):676–679.

Wood, E. R., Dudchenko, P. A., Robitsek, R. J., and Eichenbaum, H. (2000). Hippocampal Neurons Encode Information about Different Types of Memory Episodes Occurring in the Same Location. *Neuron*, 27(3):623–633.

Yartsev, M. M. and Ulanovskyi, N. (2013). Representation of Three-Dimensional Space in the Hippocampus of Flying Bats. *Science*, 340(6130):367–372.